ELECTRICAL DEMAND REDUCTION IN REFRIGERATED WAREHOUSES

by

JOY E. ALTWIES

A thesis submitted in partial fulfillment of the requirements for the degree of

MASTER OF SCIENCE

(MECHANICAL ENGINEERING)

at the
UNIVERSITY OF WISCONSIN – MADISON

1998

Abstract

Electric utilities are currently searching for ways to meet the ever-increasing demand for electricity. One available option involves reducing customer demand during the daytime and during summer months, when demand for electricity peaks. This research investigates one option for reducing the electrical demand of industrial refrigeration systems, which account for a large portion of total electric consumption. Industrial refrigeration systems are primarily used for processing and storage of perishable foods. Refrigerated warehouses may be able to utilize the thermal mass of the stored products to shift their electrical consumption to off-peak times. By pre-cooling the products during the night, the refrigeration equipment could remain idle during on-peak hours without causing significant changes in the warehouse environment. To test this type of operating strategy, a large frozen vegetable processing and warehousing facility in south central Wisconsin was chosen for this research. A literature investigation into the effect of temperature fluctuations on frozen vegetable quality indicated that the expected variations in storage temperature would not cause significant quality losses.

The study began with the development of a computer model of the test warehouse. The thermal characteristics of the stored products and the physical attributes of the warehouse structure determine the temperature changes in the warehouse under different weather conditions. The model is used to predict the temperatures inside the warehouse during any time of year and using any type of operating strategy. The model

was validated experimentally to ensure the accuracy of its results, then used to estimate the annual economic impact of implementing three possible demand shifting strategies.

Among the three options studied, full demand shifting offers the greatest savings but requires the largest amount of installed refrigeration capacity. This strategy involves a complete shutdown of the refrigeration equipment during on-peak hours. By idling the refrigeration system during the test facility's 14-hour on-peak period, the equipment must be able to remove 24 hours of heat gain during the 10-hour off-peak period. Modeling indicates that the product temperature will vary between a minimum of –12.5°F and a maximum of –2.5°F. Full demand shifting will save approximately $82,000 annually over normal operation at this facility. Other demand shifting strategies either offered minimal savings or required an unreasonably complex control system for implementation. Due to a preexisting lack of refrigeration capacity at the warehouse investigated, no operating strategies were implemented during the course of this project. An interactive spreadsheet, which calculates the economics of each demand shifting option, was created for use by warehouse operators and utility employees in future decision-making.

Acknowledgements

This document is the culmination of many long hours and late nights, and I would like to thank everyone whose input made it possible. To my project advisors, Professors Sandy Klein and Doug Reindl, I am forever grateful to have worked with both of you. Your guidance, knowledge, and patience throughout this project were always greatly appreciated. Thanks also to Professors Bill Beckman and John Mitchell for their contributions to my project, both directly and indirectly through their work in the Solar Energy Lab. I am very grateful to the personnel at Alliant Energy and Agrilink who were involved with this project. Their helpfulness and positive attitude provided encouragement and aided my progress substantially. To my project partner, Dan Dettmers, this research would have been nearly impossible without your help. Thanks for taking all those trips to the warehouse with me; we'll have to stop by the Boar's Nest for lunch again soon. I would also like to thank everyone at the Solar Lab, and especially Dave Bradley, TRNSYS engineer. You have all made the Lab a friendly, enjoyable place to learn and work, and I am convinced that Dave's vigilant firefighting is the only thing standing between us and utter technological chaos.

Finally, I want to thank my family for all they have given me. To my parents, Joe and Jeanie Jackson, thank you for the many years of unfailing support. You encouraged me to achieve great things and then gave me the self-confidence to reach those goals. My

successes are a testament to the incredible upbringing you gave me. I am proud to be your daughter.

Last but far from least, I want to thank my husband, James. I honestly don't know how I could have survived this past year and a half without you. Thank you for your patience through the months of never-ending homework, for your words of encouragement when I desperately needed them, and for reminding me there's more to life than work. I appreciate every gesture of support and encouragement you showed me (remember those late night trips to campus?). Thank you for keeping me sane and happy.

Table of Contents

List of Figures

List of Tables

Nomenclature

Area……area of doorway

D_f……... doorway flow factor

D_t……... doorway open-time factor

E……effectiveness of doorway protection device

F_m……... density factor

h_{cold}…… enthalpy of air – refrigerated side

height…… height of doorway

h_{forced}…….. heat transfer coefficient: forced convection

h_{free}…… heat transfer coefficient: free convection

h_{hot}……. enthalpy of air – warm side

h_{mixed}…….. heat transfer coefficient: mixed convection

h_{rad}……. heat transfer coefficient: radiation

h_{total}…… heat transfer coefficient: total

k……. thermal conductivity of air

k_{box}…… thermal conductivity of box

L…… length

q ..... infiltration load, per door

$Q_{ASHRAE1990}$ ..... corrected infiltration load, per door

$Q_{ASHRAE1994}$ ..... corrected infiltration load, per door

t_{box} ..... thickness of box

ρ_{cold} ..... density of air – refrigerated side

ρ_{hot} ..... density of air – warm side

Chapter 1

INTRODUCTION

1.1. Background and Purpose of Research

Electric utilities across the country are studying ways to meet the ever-increasing peak electrical demands of their customers. In many areas, utilities are faced with few options for supplying additional electricity. With deregulation on the horizon, many companies are reluctant or unable to make the large capital investments necessary to build additional generation facilities. Surrounding suppliers may be able to sell surplus power, assuming extra supply is available and transmission lines exist. Some utilities have developed rate plans that include "interruptible" service options for customers. In this case, utilities suspend service to their interruptible customers when aggregate electrical demand approaches the utility's maximum available capacity. In exchange, the customer may receive a lower overall electric rate or a lump sum payment in the event their service is suspended. These peak demands most often occur during the middle of hot summer days, when most residential and commercial air conditioners are operating. To curb this heavy midday usage, utilities often adopt rate structures that charge industrial and commercial customers a higher electric rate during peak-use periods. Under this "time-of-use" rate structure, days are divided into on-peak and off-peak periods. The cost of energy used during on-peak times (usually 12 or 14 hours during the

daytime) is greater than during off-peak times (usually nights, weekends, and holidays.) Customers may also be required to pay a monthly demand charge, which is determined by the highest instantaneous amount of on-peak power drawn by the customer during that month. Hence, it is in the customers' best interest to keep their on-peak energy use to a minimum. Inducing customers to voluntarily adopt energy conservation measures is the utility's only cost-free option. When or if these strategies are unavailable, all electric consumers may experience power blackouts.

The objective of this research project is to investigate a strategy that has the potential to significantly reduce the on-peak electrical demand associated with industrial refrigeration systems. In the U.S., the industrial sector is responsible for the largest aggregate consumption of electricity [source: Energy Information Administration]. As a result, reducing the on-peak electrical use of this sector without affecting their operations will help utilities meet their goals. Both the utility and the customer would benefit from lower on-peak energy usage and cost savings.

Industrial refrigeration applications, specifically refrigerated warehouses, are the focus of this project. Primarily used for processing and storage space conditioning, industrial refrigeration systems are significant energy consumers. These systems usually operate during the daytime when outdoor temperatures are highest and system performance is at its worst. This study was initiated to test the feasibility of using the thermal mass of the items in storage as a means to offset cooling demands. In this case, refrigeration equipment operates during off-peak hours and pre-cools the stored items. The equipment can then remain idle during on-peak times with minimal changes in the

storage environment and product temperature. Ideally, little or no initial investment by the warehouse owner or utility will be required to implement this type of warehouse operating strategy. Successful installations will result in substantial operating cost savings.

1.2. Description of Project

The first phase of this project is the development of a computer model of a refrigerated warehouse. Given any weather conditions, this model predicts the amount of heat gained by the warehouse, the amount of heat absorbed by the stored product, and the resulting air and product temperature profiles. Accurate prediction of these factors is vital in order to ensure the consistent high quality of the stored products throughout the year. To validate its accuracy, the model was compared to experimental data collected at the warehouse. Once the model correctly predicts the warehouse's actual performance, it is used to determine an operational strategy for demand shifting using the refrigeration system.

Ideally, a demand shifting strategy could be implemented at any refrigerated warehouse, independent of the type of products in storage or the temperature of the conditioned space. To test this theory, as well as to develop generally applicable demand shifting guidelines, the plan for this project included testing two warehousing facilities. One high temperature (above freezing) facility and one low temperature (below freezing) facility were to be selected based on the ownership/management's willingness to participate in the study.

1.3. Selection of Test Facilities

Work on this project began in September 1997 with the selection of a low temperature refrigerated warehouse facility in south central Wisconsin. Four individual warehouses, labeled "A" through "D", are operated at this site, which processes, packages, and stores frozen vegetables. Nominally, air temperatures in the warehouses are maintained at –5 °F. The combined warehouses are capable of holding over 50 million pounds of product at full capacity. The ownership and management of the facility were very enthusiastic about the project, and were willing to supply building blueprints, equipment and operating information, and personnel as-needed in support of the project. To date, a high temperature test facility has not been selected. Due to time constraints on the completion of this project, research on the high temperature facility is left for future study. The remainder of this investigation is directed toward the low temperature application.

1.4. Food Quality Issues

Several advantages and benefits are inherent to demand shifting, most notably cost savings for the customer and reduced on-peak demand for the utility. However, possible disadvantages include risk to the product quality, shelf life, and nutrient content. While the proposed operating strategy is designed to minimize changes in the storage environment, even minor alterations and fluctuations merit investigation of possible detrimental effects. Energy and cost savings are worthless if achieved through a method that also results in compromised product.

1.4.1. Technical Aspects of Frozen Food Quality

"Preservation of foods by freezing is an excellent method of ensuring the long term retention of original characteristics, almost unchanged, of a wide variety of highly perishable foodstuffs [IIR, p.42]." Quick frozen foods retain nutrients successfully, comparing favorably with foods processed by other techniques and even fresh market products [IIR, p.90]. Processing foods by freezing offers an array of competitive advantages, and has been steadily growing in popularity since its commercial introduction in the last century. However, freezing and subsequent storage of food is energy intensive, and diligent adherence to the basic technological principles established by the industry is necessary to maintain superior product quality. The body of food quality research spanning the previous 50 years has established 0°F (-18°C) as the upper temperature limit suitable for frozen vegetable storage. In combination with proper packaging, long-term storage at or below this limit minimizes detrimental quality changes. Desiccation, nutrient degradation, flavor or color alterations, and texture damage all inevitably occur during extended storage, but their severity is highly dependent upon storage conditions such as humidity, packaging, and temperature. In order to design storage systems that minimize these effects, a basic understanding of the mechanisms causing the changes is needed. The two best-understood and controllable processes are nutrient degradation and desiccation. Both are very important to stored frozen products. The following section provides a brief summary and explanation of these processes.

1.4.1.1. Nutrient Degradation

Among the many nutrients present in foods, frozen storage affects only a select few. These include vitamin C and some vitamins in the B group, which are water-soluble. Researchers often measure the concentration of these nutrients remaining in the food after preparation to indicate the extent of total nutrient degradation [IIR, p.90-92]. Vitamin loss occurs through two basic mechanisms: oxidation (via. enzymatic reactions) and water-soluble losses. In the presence of certain enzymes, vitamins such as vitamin C will oxidize during storage. Blanching prior to freezing combined with consistent storage below 0°F effectively inactivates these enzymes. In addition, blanching and "drip" are the two avenues by which water-soluble vitamins can exit food. "Drip" is water that has been removed from the food in the form of ice crystal formation during processing and storage. Water-soluble vitamins are present in the drip, which are then lost from the product upon preparation (assuming the water is discarded). This process of vitamin loss is only controllable by inhibiting the amount of frost formation. Unfortunately, the majority of the damage caused by this mechanism happens after retail sale of the food. According to researcher/author Amihud Kramer:

> There is good reason to believe that damage to nutrient levels in foods occurs to the greatest degree during handling and preparation of the foods in the home (Lachance et al., 1973), to a lesser extent in the retail and distribution channels, to a still lesser extent during storage, particularly at low temperatures, and to a relatively minor extent during actual commercial processing of the foods [Kramer, p.58].

Further evidence supports this conclusion. When cold storage facilities maintain temperatures at or below 0°F (-18°C), vitamin losses in their products are minor even

after storage for one year. The International Institute of Refrigeration offers this summary of the relationship between storage temperature and vitamin retention during frozen storage:

> The retention of vitamins during frozen storage varies considerably from product to product. In general it can be stated that vitamin C is rather stable over a storage period of one year in both fruit and vegetables if the product temperature is colder than –20°C/-25°C (–4°F/-14°F). In these cases losses of 10% are to be expected. At temperatures of about –30°C (–22°F) practically no losses can be observed. At elevated temperatures of –10°C/-12°C (14°F/10°F) losses of up to 80 to 90% can occur after storage for one year [IIR, p.94].

Previous studies offer unanimous results. Lower storage temperatures result in better nutrient retention. However, maintaining extremely low temperatures (below –22°F/–30°C) in frozen warehouses may be economically infeasible. Warehouse operators must strike a balance between product quality and profitability, and they often opt to operate at or near the 0°F (-18°C) maximum for frozen vegetables and meats.

1.4.1.2. Desiccation

Desiccation of foods during frozen storage is the process that causes many common quality problems. Clumping, excessive frost formation in the package, dryness, discoloration, and freezer burn are all end results of various levels of desiccation. The degree to which the desiccation occurs depends on both the caliber of the product packaging and the variations in air temperature in the storage environment. Packaging can be carefully chosen to provide protection for the product, but temperature variations within the storage space are unavoidable. Even the most advanced refrigeration

equipment cannot maintain a constant temperature at all times due to day-to-day operations of the facility (door openings, warm product entering, defrost cycles, etc.). In order to limit the effects of desiccation, the mechanisms causing it must be understood. The process of desiccation follows several steps, which are explained concisely in the following excerpt:

> 1) The layer of air between product and packaging is subject to temperature variations. As the outside temperature decreases, the temperature of the inside surface of the packaging will drop below the product surface temperature and ice from the product will sublime and condense on the inside of the package.
> 2) When the ambient temperature increases, the process is reversed and the water vapour will condense on the product surface.
> 3) As the cooling-heating cycle recurs, the crystals on the product surface tend to follow package temperature more closely than the mass of the product, and this results in further sublimation of ice from the product to the package surface [IIR, p.62].

The driving force behind the migration of moisture in the product is the saturated vapor pressure gradient between the product and the surrounding air. Frozen foods have the same saturation vapor pressure as ice at the same temperature [IIR, p.60]. Figure 1.1 shows the change in sublimation pressure (saturated vapor pressure) with change in temperature for pure ice.

Figure 1.1. Sublimation Pressure vs. Temperature for Ice

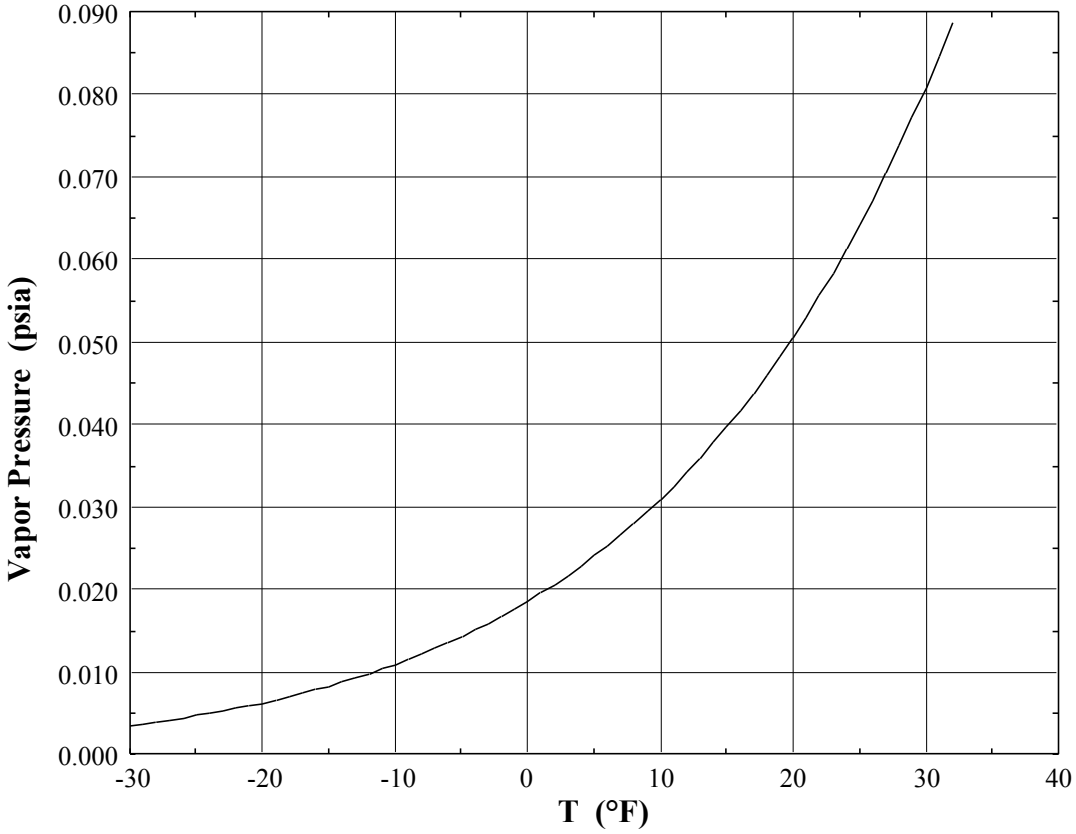

When the air temperature drops in step 1, the vapor pressure also decreases, and a gradient forms between the air and the product surface. This gradient drives the sublimation of moisture out of the product until the product cools and equilibrium is reestablished. As described in step 2, the reverse occurs when the surrounding air and packaging rise above the product temperature. The product is now the colder surface, and frost, previously deposited on the inside of the packaging, will sublime and condense on the product surface. The key to limiting desiccation due to temperature variation is to avoid temperature changes that correspond to large changes in ice sublimation pressure. The shape of the curve in Figure 1.1 indicates that the rate of sublimation will be much

greater when the average storage temperature is higher (the slope of the vapor pressure curve increases at higher temperatures). For example, a temperature variation of +/- 5°F causes a more severe fluctuation in sublimation pressure when the average temperature is 25°F (.050 psia to .081 psia) than when it is –10°F (.008 psia to .014 psia). As with nutrient loss, desiccation can be kept to a minimum by maintaining average storage temperatures as low as possible. Also, tight-fitting packaging made from vapor-impermeable materials can effectively halt frost formation by eliminating the layer of air inside the package.

1.4.2. Effect of Demand Shifting

For this study, the effect of temperature fluctuations on product quality is of particular relevance. No direct investigation of demand shifting effects on food quality was conducted during the course of this project, but an extensive literature search revealed several related studies. Previous investigations involved a variety of food products (spinach, cauliflower, peas, strawberries, and more) and were originally undertaken for reasons ranging from food quality deterioration to energy savings. Each study investigated the effect of temperature fluctuations over ranges of interest for each particular project. Those studies that never allowed their frozen products to exceed 32°F (0°C) throughout the study consistently obtained results showing little to no degradation attributable to the fluctuations in storage temperature. The studies allowing extreme temperature fluctuations with freeze / thaw cycles reported significant quality losses. Table 1.1 summarizes the results of several investigations. This evidence is presented

primarily to dispel some existing generalizations often made regarding the effect of temperature variations during storage. It is not, however, meant as an all-encompassing endorsement of the use of fluctuation-causing operational techniques in every situation. The research presented here is strictly applicable to vegetable (and meat, in one case) tissue. Extending these results to other frozen products, such as breads and ice cream, would be ill advised. Additional research, preferably in the form of both a literature search and a direct investigation, is necessary before any conclusions can be drawn about quality effects on other products.

Table 1.1. Summary of Previous Frozen Food Quality Research

Product	Investigator	Conditions	Freeze / Thaw?	Summary
Cauliflower	Aparicio-Cuesta & Garcia-Moreno (1988)	-8°F (10 hrs) to 39°F (14 hrs) for 10 days, sealed in polyethylene bags	YES	Vitamin C losses of 35 % over control, no color change, loss of flavor, softer
Strawberries, blackberries, raspberries, peaches	Woodroof & Shelor (1947)	-20°F to 0°F and 0°F to 10°F for up to 12 months, raspberries in sealed 3-lb metal cans, peaches in 1-lb waxed cartons, strawberries and blackberries in 10-lb moisture-proof bags inside corrugated boxes	NO	Color, flavor, & aroma of low-temp cycled strawberries "only slightly less pleasing" than those at constant -10°F, differences in blackberries were less than with strawberries, peaches more sensitive to fluctuations, high-temp fluctuations worse than constant 10°F in most cases
Snap beans, corn, peas, strawberries, raspberries, cantaloupe	Hustrulid & Winter (1943)	-20°F to 0°F (12 to 24 hrs) for minimum of 6 months, unknown packaging	NO	No influence on appearance or palatability compared with control group at constant temperature
Peas (4 varieties)	Boggs, et al. (1960)	-5°F to 5°F, -10°F to 10°F, and 0°F to 20°F (24 hr sinusoidal cycling), "retail" packaging	NO	Fluctuation of temperature *per se* had little or no effect on deterioration
Pork roasts, strawberries, snap beans, peas	Gortner, et al. (1948)	0°F (6 days) to 20°F (6 days) for 1 year, wrapped in cellophane (pork) or commercial packaging	NO	Quality changes were equivalent to control foods held at constant 10°F
Okra, peas, strawberries	Ashby, et al. (1979)	-11°F (12 hrs) to 0°F (12 hrs) for 1 year, plastic pouches or paperboard cartons placed inside corrugated boxes	NO	No significant changes

As will be shown later in this report, the product temperature fluctuations expected from a full demand shifting strategy are comparable to the study by Ashby, et al. (-12.5°F to -2.5°F maximum range), and product temperatures are required to stay below 0°F. Minimum packaging used at this facility includes a layer of heavy-duty corrugated cardboard with a polyethylene liner. Considering these factors, results similar to those obtained by Ashby, et al. are expected. Nutrient retention is expected to remain the same or even improve, due to the decrease in average storage temperature from the set point of –5°F to –7.5°F. The research by Kramer (1979) indicates that the periodic temperature variations will not affect nutrient loss.

The following chapters outline the development of computer models for the warehouse, as well as experimental validation and demand shifting strategy investigation completed during the course of this research.

Chapter 2

PRODUCT MODEL: FINITE ELEMENT ANALYSIS

2.1. Purpose of Model

Full demand shifting requires idling the refrigeration equipment in the warehouse for the entire on-peak period, typically 10 to 14 hours in length. Computer modeling offers the opportunity to predict the effect of "floating" the refrigerated warehouse for these hours. The first stage in the development of a total warehouse model is the creation of the product model. This phase, which is described fully in this chapter, models the thermal interaction between the stored product and its surroundings using finite element analysis.

2.2. FEHT: Finite Element Heat Transfer

To predict the thermal performance of the stored products, a model of the items in storage was developed using finite element software called FEHT (Finite Element Heat Transfer) [Klein et al., 1995]. FEHT allows the user to create a two-dimensional representation of the system to be modeled. In this case, a drawing of frozen vegetables arranged in stacked boxes was produced, then discretized into many individual elements. Given the properties of the material and the conditions on its surfaces, FEHT calculates the distributed temperature response of the material over the specified time period.

2.3. Storage Layout and Model Representation

In the low temperature warehouses, frozen vegetables are stored in large bulk boxes or in cases for shipping. Warehouses "A", "B", and "C" hold bulk storage boxes, which are each approximately 64 ft^3 in volume and constructed using heavy-duty cardboard. A plastic liner is used inside the boxes as an additional vapor barrier for the frozen product. Warehouse "D" holds cased goods prior to shipment for retail sale. The frozen product in this warehouse is packaged inside 1-lb bags or small boxes like those available in grocery store freezers. These individual containers are packed into small (approximately 2'x1'x1') cardboard boxes, which are then arranged onto 4'x4'x8' pallets. To maintain these stacked arrangements during movement, the pallets are wrapped in an additional layer of plastic. The extra packaging in warehouse "D" serves as an additional protective barrier for the frozen product, making it less susceptible to the temperature variations inherent to demand shifting. Figure 2.1 shows the model created to represent the stacked boxes and cases. The model block depicts five vertical stacks of bulk-boxed vegetables in a compact arrangement, allowing no air movement between the boxes. Each vertical stack is six boxes high, matching the real arrangement in the bulk storage warehouses. This situation, in which all of the boxes are stored tightly packed together, symbolizes the thermally worst-case scenario. Arranged in this manner, the warehouse air contacts the smallest possible surface area of the boxes. Thermal interaction between the air and product is reduced, so the air must absorb more of the heat gained by the warehouse. The result will be higher warehouse air temperatures.

Figure 2.1. Basic Frozen Vegetable FEHT Model

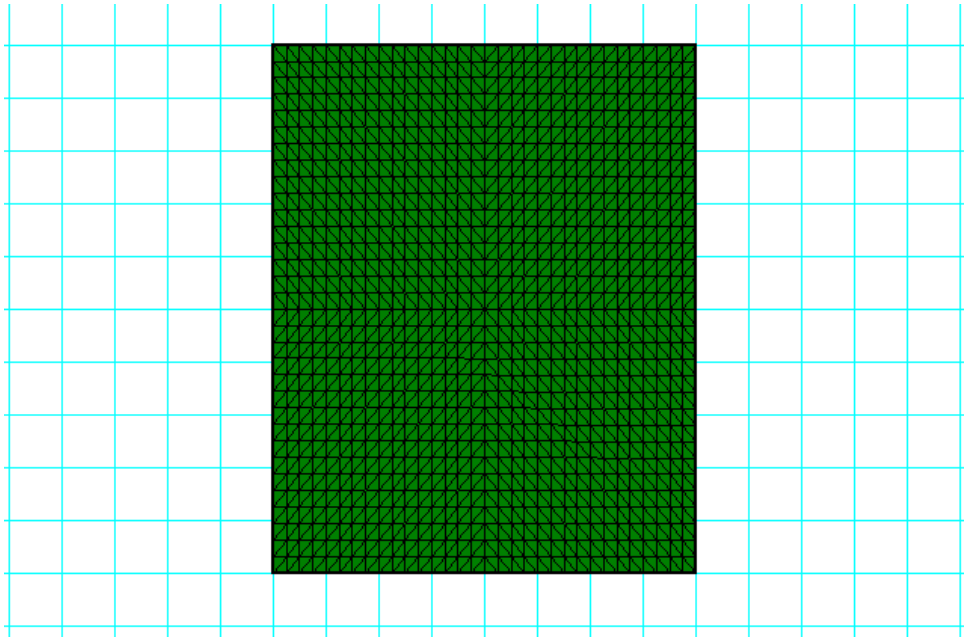

This situation is a reasonable representation of the actual stacking arrangement used in warehouses "A", "B", and "C". In warehouse "D", metal racks are used to hold the product pallets and allow more air movement between pallets. However, to make the most conservative estimate of the warehouse performance, the compact arrangement was used in the product model for all warehouses.

2.4. Required Inputs

2.4.1. Properties of Product

FEHT solves the system of equations using a linear finite element method to predict the temperature and heat flow at all locations in the block. However, several inputs must be provided to execute the calculations. First, the thermal properties of the

material must be provided to the program. These properties include density, thermal conductivity, and specific heat. Because the warehouse facility stores a wide array of frozen vegetables, the property values chosen must be reasonably representative of the entire group. Table 2.1 gives information about six vegetables stored at this facility. Collectively, these six vegetables comprise 86.7% of the product stored in the bulk warehouses and 56.4% of all cased products, and their thermal properties were used to represent the whole. Unfortunately, the available property data specific to frozen vegetables is somewhat limited. Information was collected from both the International Institute of Refrigeration and the 1993 ASHRAE (American Society of Heating, Refrigerating, and Air Conditioning Engineers) Fundamentals Handbook, which lists the thermal properties of various foods. The most recent edition of the Fundamentals Handbook, 1997, does not include this information, which will be included in the 1998 Refrigeration Handbook instead. Table 2.2 shows the data collected from the aforementioned sources. The average value for each property was used in the FEHT model. Property data for air, ice, and water are also included as a reference. The most difficult value to obtain was bulk density, which varies widely depending on the type of product, the size of the individual pieces, and the packing density. For example, chopped frozen broccoli has a much lower bulk density than frozen strawberries in syrup. The irregularities of the broccoli allow for greater air spaces between the individual pieces when placed in packaging. The strawberries, on the other hand, allow virtually no air space. For the FEHT model, a value close to the single available reference for shelled peas was used. The bulk density of peas, which is itself variable depending on the size of

the individual peas, is a good median value to represent the range of products in storage. The value of 43.7 lb/ft^3 (700 kg/m^3) is the bulk density of peas corresponding to the given thermal conductivity of 0.3178 Btu/hr-ft-R (0.55 W/m-C) [IIR, p.52]. The effect of ranging these inputs on the total outcome of the model is discussed in section 4.4, Sensitivity Analysis.

Table 2.1. Storage Information for Six Frozen Vegetables

Vegetable	Bulk (% of total)	Cased (% of total)	Bulk Mass (lbm)	Cased Mass (lbm)
Baby Lima Beans	4.2	---	4905	---
Broccoli	2.8	3.5	33136	16363
Carrots	10.7	3.3	126774	15441
Corn (cut & cob)	39.1	23.9	460631	112581
Green Beans	10.3	10.8	122034	50787
Peas	19.6	15.0	231405	70410
Total	86.7	56.4	978885	265582

Table 2.2. Property Data

Vegetable	% Water (mass)	% Water Frozen @ -4°F (-20° C)	Specific Heat below freezing (Btu/lb-F)	Density (lbm/ft^3)	Thermal Conductivity (Btu/hr-ft-R)
Baby Lima Beans	67		0.401		
Broccoli	90		0.471		0.223
Carrots	88	94	0.465		0.387
Corn (cut & cob)	74		0.423		
Green Beans	89		0.468		
Peas	74	89	0.423	43.7	0.3178
Average	80	92	**0.442**	**43**	**0.309**
Air			0.240	0.087	0.013
Ice			0.466	57.4	1.41
Water			NA	62	0.034

2.4.2. Boundary Conditions

The second input required before calculating temperature distributions using the model is boundary conditions on the surfaces of the product block. A heat transfer coefficient and an air temperature are needed to represent the interaction between the boxed product and the surrounding air. The following two sections describe the process used to determine these model parameters.

2.4.2.1. Determination of Heat Transfer Coefficient (h_{total})

Heat transfer between the product surface and the warehouse air occurs through free convection, forced convection, and radiation. The combined effect of these three components, in addition to the resistance offered by the product packaging, is represented by an average heat transfer coefficient. The basic procedure used to calculate the average heat transfer coefficient involves several steps. First, the coefficients for free and forced convection are calculated separately using Nusselt number correlations, then combined according to the following equation [Incropera and DeWitt, p. 524]:

$$\left[\frac{(h_{mixed} * L)}{k}\right]^3 = \left[\frac{(h_{free} * L)}{k}\right]^3 + \left[\frac{(h_{forced} * L)}{k}\right]^3$$

The total heat transfer coefficient on the surface of the box is then determined by combining the mixed convection coefficient with the radiation coefficient and box resistance. On the inner surface of the box, the product is assumed to be in contact with the packaging with negligible contact resistance. The convection and radiation

coefficients combine in parallel, then in series with the box resistance to give the desired result:

$$\left(\frac{1}{h_{total}}\right) = \left(\frac{1}{h_{mixed} + h_{rad}}\right) + \left(\frac{t_{box}}{k_{box}}\right)$$

All variables are defined in the Nomenclature section included before chapter 1.

Originally, two total heat transfer coefficients were used. Presumably, during on-peak hours, the fans in the storage areas would remain idle. In this situation, the convection coefficient would not include the forced convection component during the hours from 8 AM to 10 PM. The calculated values for the total heat transfer coefficient would be approximately 0.80 Btu/hr-ft^2-F during the 10-hour off-peak period and about 0.67 Btu/hr-ft^2-F during the 14-hour on-peak period due to the reduced air movement during the on-peak hours. Turning on the evaporator fans at night increases the air movement, which causes an increase in the heat transfer coefficient. However, to simplify the input to FEHT and speed calculations, a constant value of 0.75 Btu/hr-ft^2-F was used. Like the food property values, the overall effect of increasing or decreasing this value is discussed in Sensitivity Analysis, section 4.4. The detailed calculations, Nusselt number correlations, and solutions to the equations discussed are included in Appendix A.

2.4.2.2. Air Temperature

The air temperature inside the warehouse is a required input for the FEHT model. However, both the air velocity on the outside of the boxes (needed for the heat transfer

calculations of section 2.4.2.1) and the air temperature inside the warehouse are unknown. In fact, the air temperature is one of the outputs from the total model that is being sought. Without field data, a worst-case estimate for the air velocity was chosen to be 600 ft/min and the air temperature was varied from an initial value of –5°F up to 60°F over a 24-hour period. By arbitrarily imposing these boundary conditions, the FEHT model could be run. The results offered by these inputs do not correlate to any real situation which would occur in the warehouse, but instead offer the opportunity to view the relative temperature variations within the stacked boxes of product.

2.5. Results

Figure 2.2 shows the color-banded temperature contours in the vegetables. Because these results were calculated using estimated worst-case values, the results are only meaningful as a means of locating the areas of the product most severely affected by a change in the air temperature. The figure shows that the corners and edges are the most affected, while the center of the stack experiences no change in temperature at all. The outcome indicates that product stored on or near the edges of the stacks is of the greatest concern as the warehouse air temperature rises during the on-peak period. This initial result corresponds to observations made by several previous researchers, most notably Ashby, et al. (1979). Their data confirmed that the most exposed products (those near the edges and corners of the arranged boxes) were more affected by temperature variation than product stored on the interior of the stacks.

Figure 2.2. FEHT Temperature Variation Results: Worst Case Locations

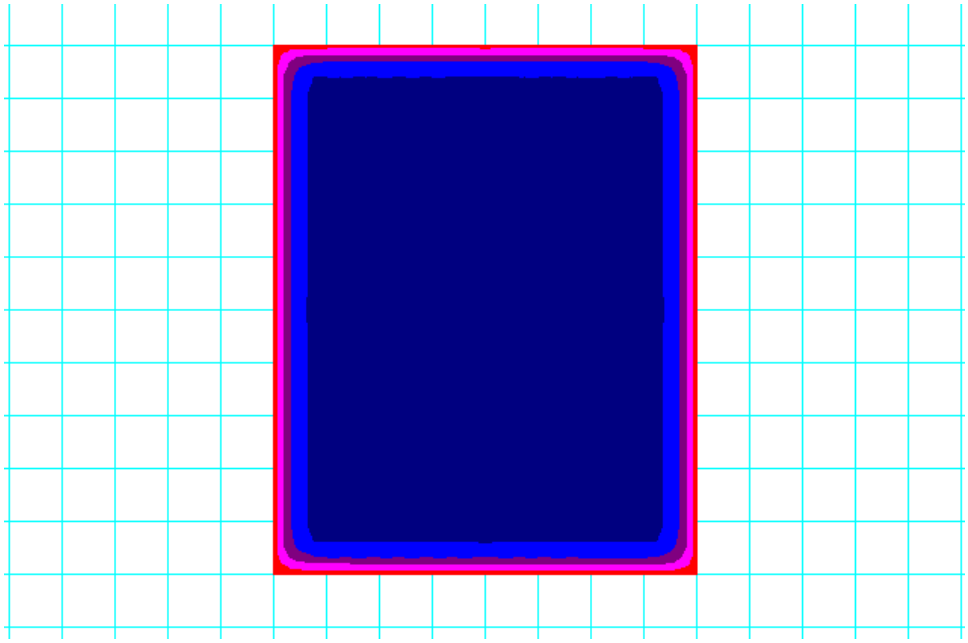

Chapters 3 and 4 explain the further development of a complete warehouse model. By adding additional components and incorporating the warehouse cooling load into the working product model, the need for guess values in the calculations is eliminated.

Chapter 3

WAREHOUSE MODEL: COOLING LOAD ANALYSIS

3.1. Purpose of Model

In addition to the development of a model that predicts the thermal performance of stored products, the cooling load in the warehouse must also be modeled to calculate

the air temperature rise during the on-peak period. The warehouse cooling (or refrigeration) load is a measure of the rate at which energy enters the refrigerated space over a given time period. The largest cooling load, known as the design load, typically occurs when the outdoor air temperature, humidity, and solar radiation are highest. For the low temperature warehouse, the design conditions were estimated to be an unusually warm, sunny July day for Madison, Wisconsin. Unlike the product model, a single cooling load model is not sufficient to properly represent the thermal performance of the four warehouses located at the facility. Three distinct models for warehouses "C", "D", and "A" & "B" together were created for reasons that are discussed in the following sections.

3.2. Components of Total Cooling Load

The total cooling load consists of five general categories: transmission load, product load, internal load, infiltration load, and equipment load. Figure 3.1 graphically illustrates the components of the total cooling load, which are explained in detail in the following sections.

Figure 3.1. Components of Warehouse Cooling Load

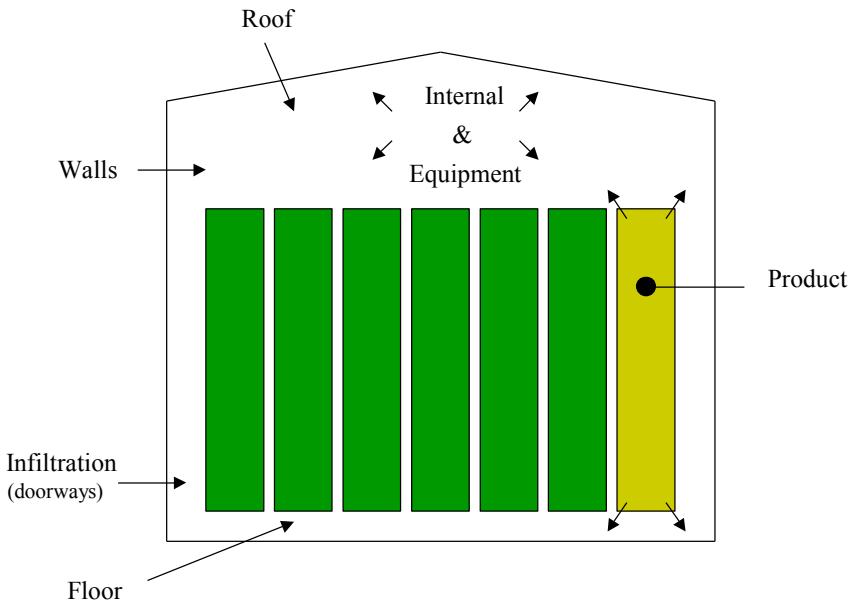

3.2.1. Transmission Load

Transmission load is defined as the rate of energy transfer through the walls, roof, and floor of a conditioned space. Throughout the day, the outdoor air temperature varies hour-by-hour. The rate of heat gain through the roof and walls is determined knowing the orientation of the surface (facing south, for example), the outdoor air dry-bulb temperature (adjusted to include the effects of solar radiation hitting each outer surface), the indoor air set point temperature, and the overall heat transfer coefficient (i.e. U value) of the surface. Additional gains occur through the floor due to a glycol heating loop that is imbedded in the concrete. The glycol loop system prevents freezing and eventual heaving of the ground beneath the warehouse. To calculate the rate of heat gain through every surface, the conditions on the exterior of the surface (outdoor weather, adjoining

room temperature, etc.) and information about the warehouse structure are needed. Basic information about the construction of the warehouses was obtained using blueprints provided by staff at the facility. Warehouses "A" & "B" were built together during the 1960's, with identical construction. As a result, a single cooling load model was created for both. However, warehouses "C" and "D" were constructed separately within the last 15 years. The building materials used in the walls and roof were different from "A" and "B" and from each other, requiring the creation of a separate model for each. Table 3.1 gives some basic information about each warehouse for simple reference.

Table 3.1 Warehouse Information

	Warehouse "A" & "B"	Warehouse "C"	Warehouse "D"
Size (ft^2)	99,069	25,963	79,869
U Value -- Walls (Btu/hr-ft^2-F)	0.036	0.046	0.046
U Value -- Roof (Btu/hr-ft^2-F)	0.036	0.035	0.035
Product-to-Air Volume Ratio	0.525	0.694	0.396
Installed Evaporator Capacity (tons)	80	120	319

Modeling the construction of the buildings as carefully as possible is very important in obtaining accurate results. Material types, wall layer thicknesses, and the order of wall layers all have a strong impact on a structure's hourly transmission load profile. For example, a building constructed primarily from insulation will have a smaller thermal capacity than a building constructed mainly using concrete. As a result, the interior of the all-insulation structure will be affected more quickly by changes occurring on the exterior than the more thermally massive concrete structure. The maximum load will occur earlier in the day and daily fluctuations in the load will be

greater for the lightweight structure. A comparison of the construction and thermal performance of warehouses “A”, “B”, and “C” illustrates these effects. Warehouses “A” & “B” are constructed primarily of insulation, whereas warehouse “C” was built using prefabricated concrete and insulation walls. Diagrams of the wall and roof cross-sections for the warehouses are shown in Figures 3.2 and 3.3. Subjected to the hourly exterior surface temperatures shown in Figure 3.4, the resulting rate of heat gain through the walls and roof of warehouses “A”, “B”, and “C” are shown in Figures 3.5 and 3.6.

Figure 3.2. Cross-Section of Walls and Roof: Warehouses “A” & “B”

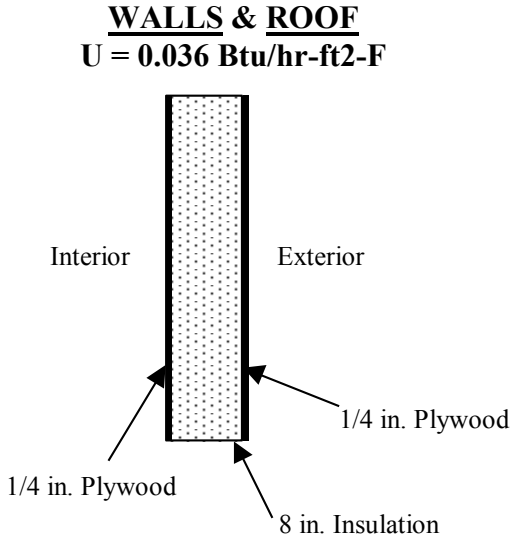

Figure 3.3. Cross-Sections of Walls and Roof: Warehouse "C"

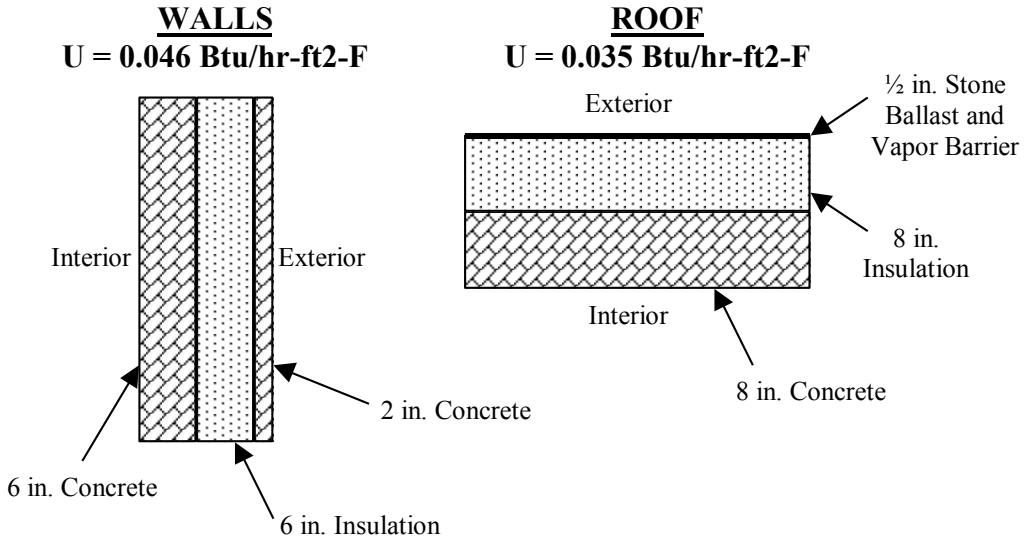

Figure 3.4. Exterior Surface Temperatures over 24 Hours: Design Conditions

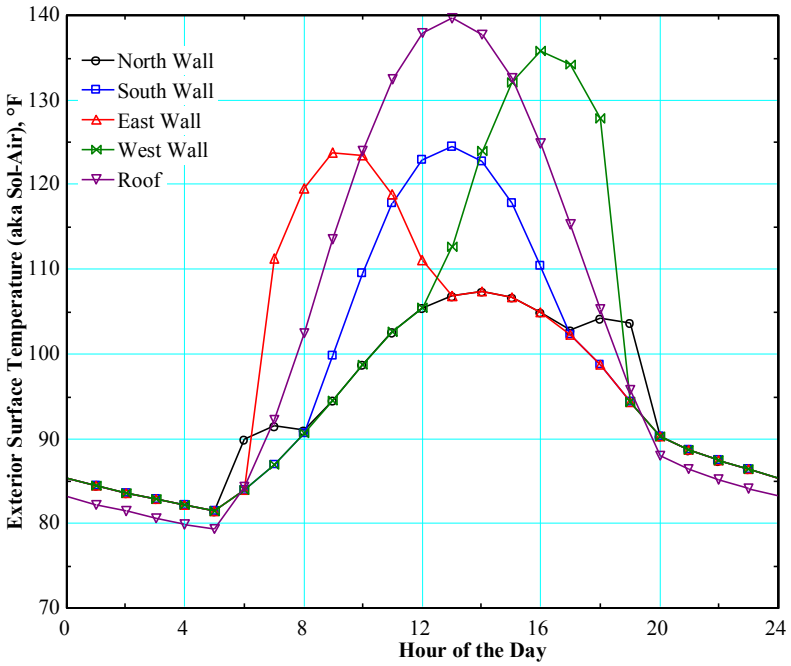

Figure 3.5. Warehouses "A" & "B": Heat Flux

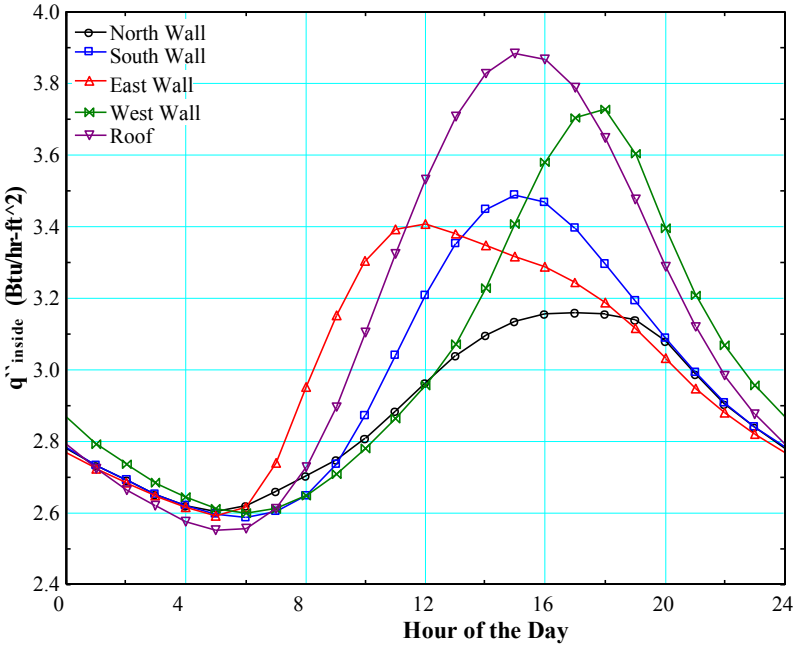

Figure 3.6. Warehouse "C": Heat Flux

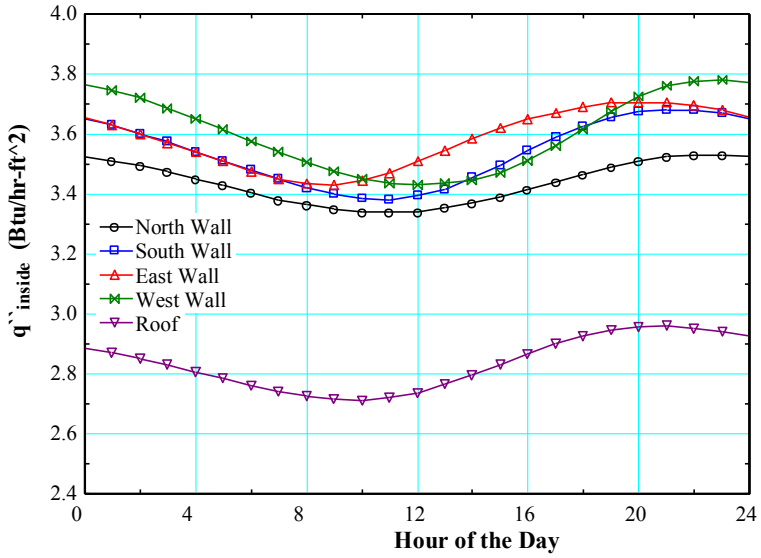

The walls and roof of warehouses "A" & "B" have identical, lightweight construction. By contrast, the construction of warehouse "C" combines concrete and

insulation, making it more massive than warehouses “A” & “B”. Unlike warehouses “A” & “B”, the roof of warehouse “C” differs from the walls. The roof contains the same basic materials as the walls, but with an additional two inches of insulation. The effects of each of these construction details are evident in Figures 3.5 and 3.6. Comparing Figures 3.4 and 3.5, warehouses “A” & “B” show only minor delays between the exterior conditions and the rate of energy passing through the walls and roof. The east wall peaks earliest, then the south wall, then the west wall. This pattern mimics the path of the sun throughout the day. The north wall shows the smallest heat gains while the roof shows the highest, again due to the positioning of the sun. By comparing these results with Figure 3.6, the effects of heavier weight concrete construction are evident. In general, the amplitudes of the daily heat flux cycles are smaller, and the peaks are shifted later into the evening due to the higher thermal capacitance of concrete. Because the roof of warehouse “C” and the walls and roof of warehouses “A” & “B” have nearly identical U values, a direct comparison of these plots can be made to determine the effect of more massive construction. The lower heat flux through the roof in Figure 3.6 is attributable to the additional two inches of insulation in the roof of warehouse “C”. The noticeable difference between heat flux of the roof and walls in warehouse “C” demonstrates the importance of modeling a building’s construction accurately.

The transmission portion of each warehouse’s cooling load was calculated using a finite-difference method for two-dimensional transient conduction through a wall. The equations were solved using EES (Engineering Equation Solver) [Klein and Alvarado,

1996]. The equations and solutions are included in Appendix B, including the equations used to calculate the exterior surface temperatures.

3.2.2. Infiltration Load

Infiltration is the uncontrolled exchange of non-conditioned air with the conditioned warehouse air through doorways or other openings. Whenever a doorway into the warehouse is opened, heavier refrigerated air spills out into the adjoining space, and warm, moist air rushes in to replace it. This air exchange adds both sensible (temperature-related) and latent (moisture-related) loads to the space. To estimate these loads, the size of the passageway, open (dwell) time, and temperature difference between the adjoining spaces must be known. When available, the facility supplied doorway timer settings for each automatic door. This information, along with on-site observations of traffic through each doorway, was used to estimate frequency of door openings and dwell times. Originally, this information was used to calculate the total infiltration load using the 1994 ASHRAE Refrigeration Handbook [ASHRAE, 1994]. However, grossly unrealistic results were obtained upon first attempting this method. A more in-depth investigation was undertaken to estimate reasonable values and possibly determine the cause of the false results. During the experimental validation of the model (discussed in section 4.3), air velocity measurements were taken in an open doorway leading into the warehouse. The readings were recorded at regular intervals along the height of the doorway and were used to create an air velocity profile. This velocity profile was then used to determine the extent of warm air exchange occurring during the open time of the

door. Knowing the mass flow rate of air into the warehouse and the difference in enthalpy between the warm and cold air, the infiltration load was calculated and compared with the results obtained from both the 1990 and 1994 ASHRAE Refrigeration Handbook methods for a like-sized doorway. An additional method originally derived by Jones and applied by Cole (1987) was also compared to the experimental results and ASHRAE calculations. The 1990 ASHRAE method gave estimates most closely resembling the experimental results. As a result, the total infiltration load for the warehouse cooling load model is calculated using the method described in chapter 27 of the 1990 ASHRAE Refrigeration Handbook [ASHRAE, 1990] for infiltration by air exchange. The basic equations used in the two ASHRAE methods are shown below. The definition of variables is included in the Nomenclature section.

$$Q_{ASHRAE1990} = q * D_t * D_f$$

$$Q_{ASHRAE1994} = q * D_t * D_f * (1 - E)$$

$$q = \left[795.6 * Area * (h_{hot} - h_{cold}) * \rho_{cold} * \left(1 - \frac{\rho_{hot}}{\rho_{cold}} \right)^{1/2} \right] * (32.17 * height)^{1/2} * F_m$$

The newer method presented in the 1994 ASHRAE Refrigeration Handbook differed from the older, 1990 method by a factor of (1-E), where E is the effectiveness of the doorway protective device. The value of E can range from 0 for no protection to 1 for perfect protection. In the original infiltration load calculation, a value of approximately 0.85 (corresponding to modern, well-sealed doors) was erroneously used in the calculation, since the air exchange occurs while the doors offer no protection at all (they

are wide open). The 1990 method, which does not include the (1-E) factor, gives results equal to the 1994 method when the value of E is 0. The meaning and correct application of the E factor was not readily apparent, so the 1990 method was used instead. A program was written to calculate and sum the results for each door opening into the four warehouses using EES and is included in Appendix C.

3.2.3. Product Load

Product load is the rate of energy transfer to the refrigerated space due to the entrance of warm product. After processing or transport, boxed frozen food between 0 and 10°F is brought into the storage area. As the newly stored product cools down to the set-point temperature of the refrigerated space, heat is released. Thus, cooling of this product is an additional load on the refrigeration system. The warehousing facility provided information regarding the amount of warm product that is brought into the warehouses each hour. The heat gain per hour is the mass of the product entering per hour times its bulk specific heat, multiplied by the difference in temperature between the storage space and the entering product temperature.

3.2.4. Internal Load

People, lights, forklifts, and other miscellaneous heat-generating objects within the refrigerated space comprise the internal load. Again using information supplied by the warehouse staff, the total heat added by each of these items was calculated. With knowledge such as the wattage and number of lights, number of forklifts, and number of workers inside the warehouses during an average hour, the heat gains were determined.

Whenever exact information was unavailable, an industry load estimating manual [Krack, 1992] was used to approximate values such as the horsepower of forklifts, gains due to intermittent occupancy by workers, and heat equivalents for electric motors. The only load-producing objects within the storage area that are not considered part of the internal load are the components of the refrigeration system itself. Heat generated by this equipment is categorized as "equipment load", which is discussed in the next section.

3.2.5. Equipment Load

The fifth component of refrigeration load is attributable to equipment. Any heat generated in the space by the refrigeration equipment itself, such as evaporator fans, is included in this category. Defrost cycles also generate heat and are a part of the equipment load. All necessary information about the operation of the equipment was supplied by the facility staff and used to calculate this portion of the total cooling load. The outcome was added to the results from the previous four components using a spreadsheet. The following section discusses the cooling load results for each warehouse.

3.3. Results for Design Conditions

Figures 3.7 through 3.10 give information regarding the total warehouse cooling load. Figures 3.7, 3.8, and 3.9 show the hourly variation of the calculated cooling load for each of the four warehouses. While the models are as accurate as possible, the calculations require additional assumptions and generalizations. Factors including the number of door openings in a given day (affecting the infiltration load) and the amount of

time a worker spends in the storage area (affecting the internal load) are variable and hence difficult to predict. As a means of gauging the accuracy of the cooling load models prior to experimental validation, the results for warehouses "A", "B", and "C" are compared to a typical warehouse of the same size in Figure 3.10, as listed in chapter 25 of the 1990 ASHRAE Refrigeration Handbook [ASHRAE, 1990].

Figure 3.7. Total Refrigeration Load for Warehouses "A" & "B": Design Conditions

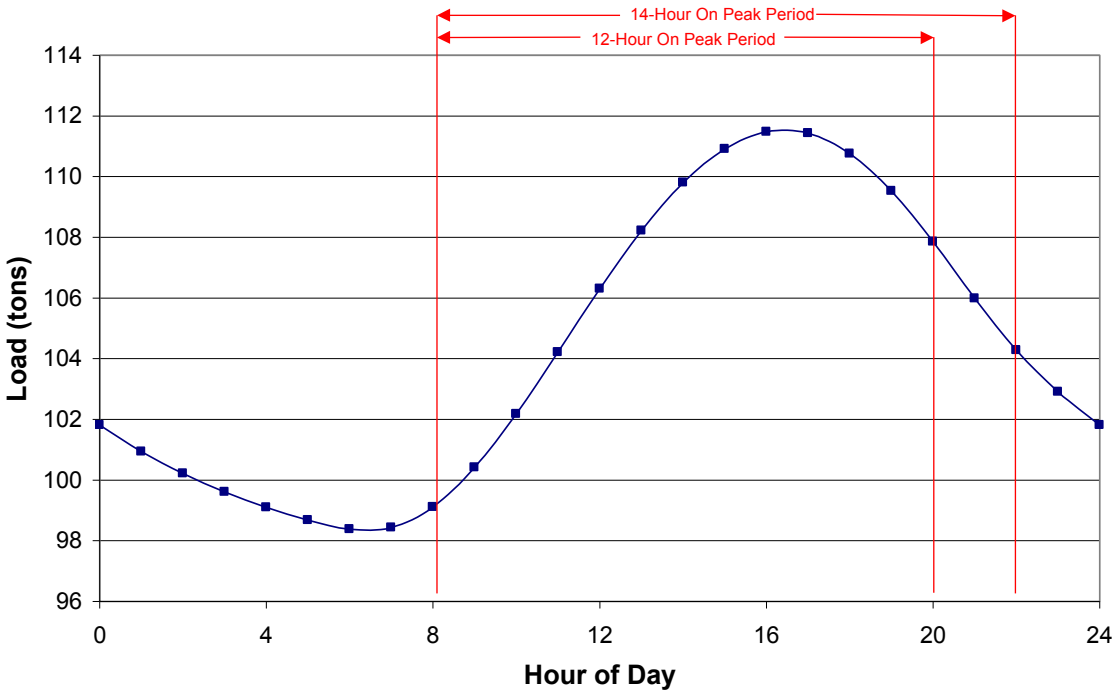

Figure 3.8. Total Refrigeration Load for Warehouse "C": Design Conditions

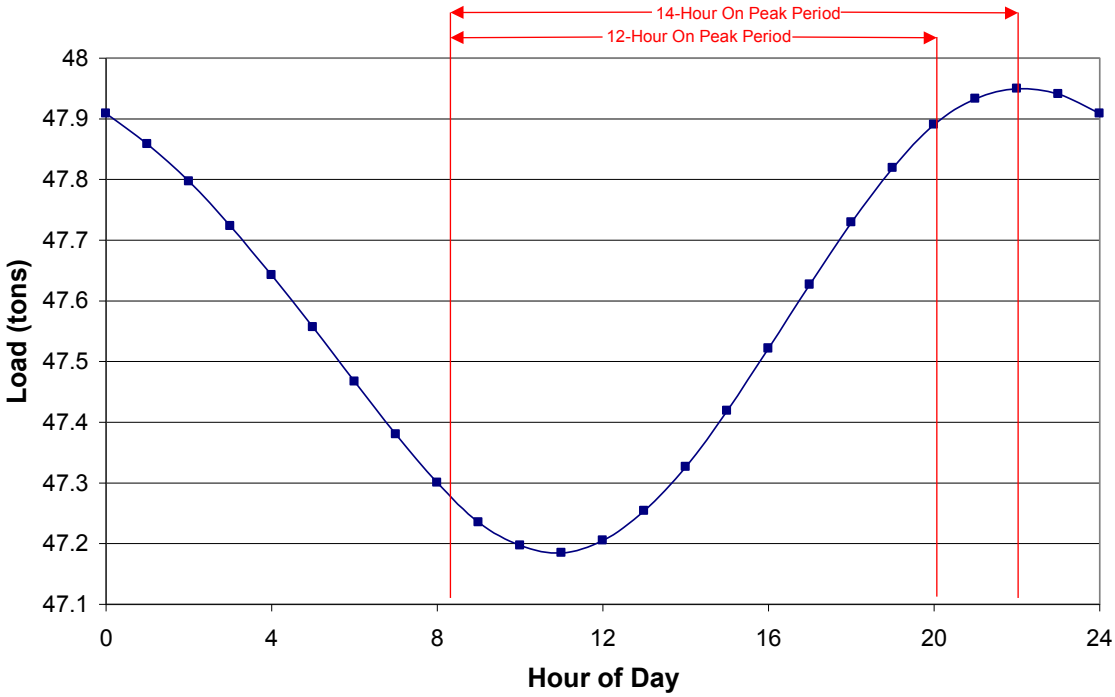

Figure 3.9. Total Refrigeration Load for Warehouse "D": Design Conditions

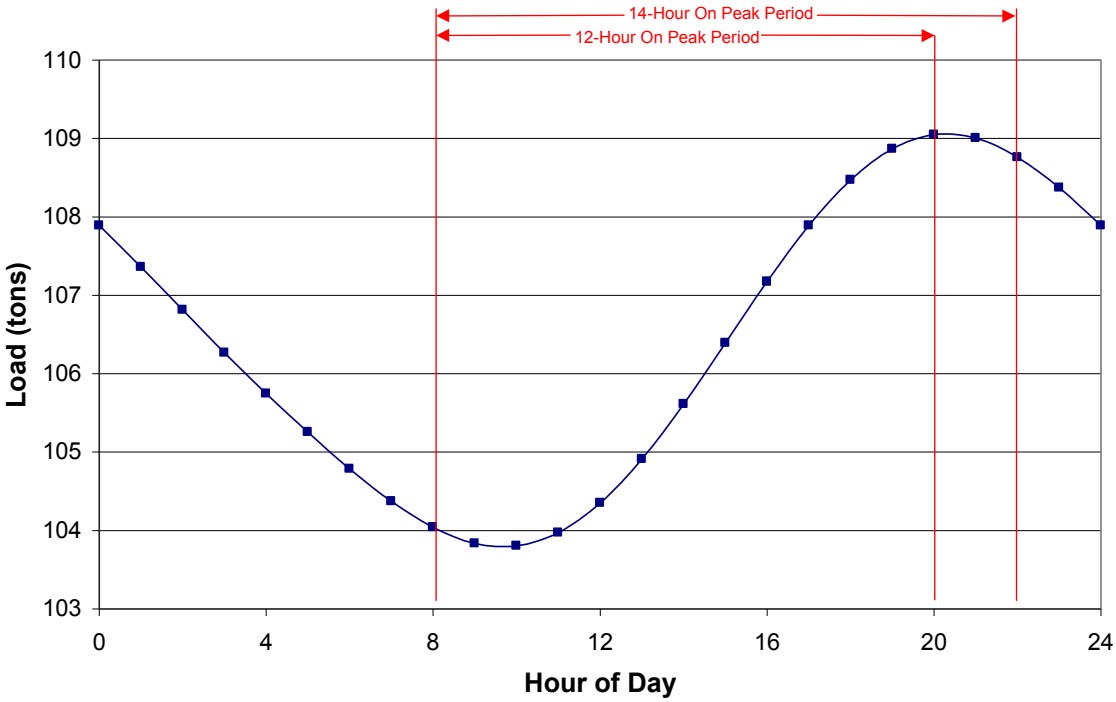

Figure 3.10. Warehouse Cooling Load Comparison (125,000 ft^2 facility)

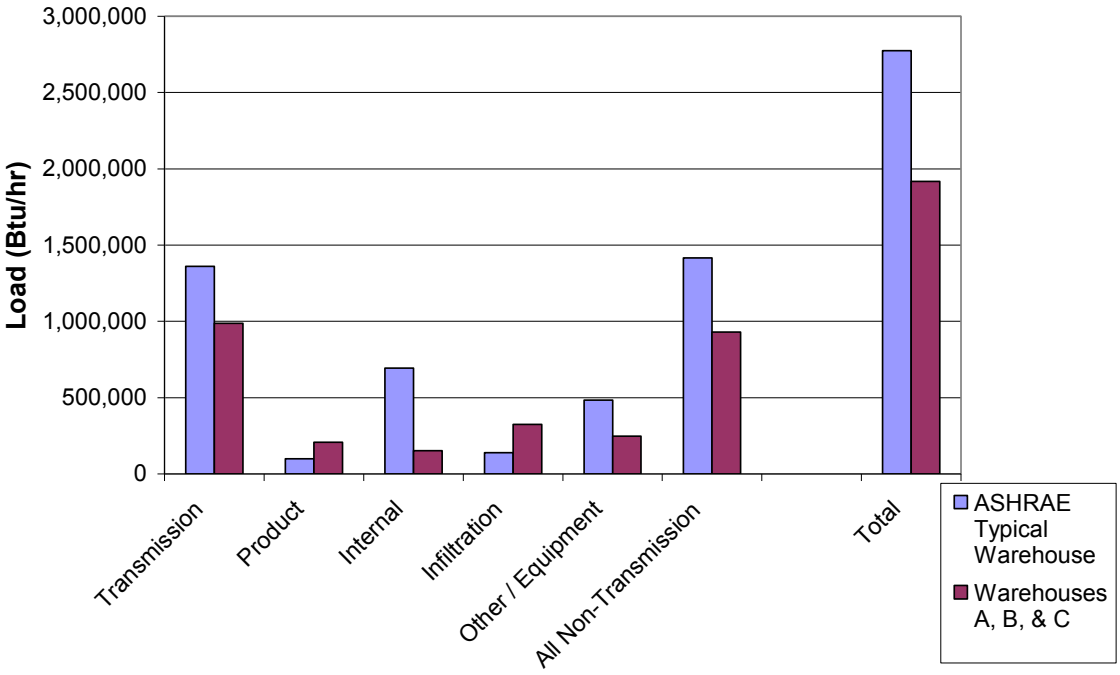

Comparison of the warehouses in Figure 3.10 indicates that the calculated warehouse has a lower total load than a "typical" warehouse of the same size. Quality construction undoubtedly contributes to the favorable transmission load comparison, and management techniques designed to minimize internal loads likely add to the significant difference. As will be discussed in the next chapter, experimental validation at the facility confirmed the loads calculated and shown in Figure 3.10.

Chapter 4

DEVELOPMENT OF COMBINED WAREHOUSE MODEL

4.1. Combined Warehouse Model

The final step in modeling the warehouses involves combining the product and cooling load models presented in chapters two and three. Like the product model, this is accomplished using FEHT software. The original model of the product is retained, but a representation of the warehouse itself is drawn around it. This addition includes a "block" of air and the outer structure of the warehouse. The whole model is carefully scaled to the actual dimensions of the facility, including the product-to-air volume ratio and the wall layer thicknesses. Figure 4.1 shows this combined FEHT model for warehouses "A" and "B".

Figure 4.1. Combined FEHT Model: Warehouses "A" & "B"

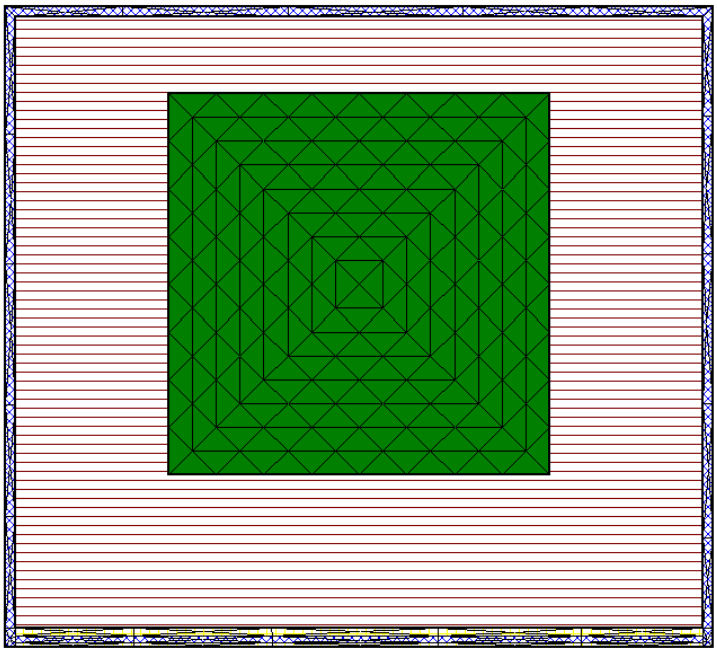

The design of the new, combined models was selected to facilitate the incorporation of the warehouse cooling load reviewed in chapter 3. The previously calculated load is applied to the new warehouse FEHT model by separating the transmission load from the remainder of the total refrigeration load. The transmission portion of the cooling load must be treated separately, because its value is dependent on the difference between the variable exterior temperature and the now-changing warehouse air temperature. The hourly values for the transmission load calculated in the previous chapter assumed a constant interior warehouse set point temperature of –5°F. In reality, however, the rate of energy flowing through the walls, roof, and floor decreases as the temperature inside the warehouse rises. To accurately portray this phenomenon and model each warehouse as a whole, all non-transmission loads are applied to the model as internal heat generation (per

unit volume of air) in the volume of air surrounding the stored product. The exterior surfaces of the warehouse are modeled with a heat transfer coefficient and surface temperature. The heat transfer coefficient of 2.9 Btu/hr-ft^2-F (17 W/m^2-K) is a standard value listed in chapter 28 of the 1997 ASHRAE Fundamentals handbook for exterior convection and long-wave radiation. The temperature used is the exterior surface temperature discussed in chapter 3. A constant temperature boundary condition of 67.5°F is assumed for the floor, which is the average of the supply and return glycol temperatures. With the material properties of each wall, roof, or floor layer known and entered into the model, the transmission portion of the load is calculated internally in FEHT. Figure 4.2 shows a simple calculation flow diagram, indicating the inputs to the final combined model and the resulting output.

Figure 4.2. Calculation Flow Diagram

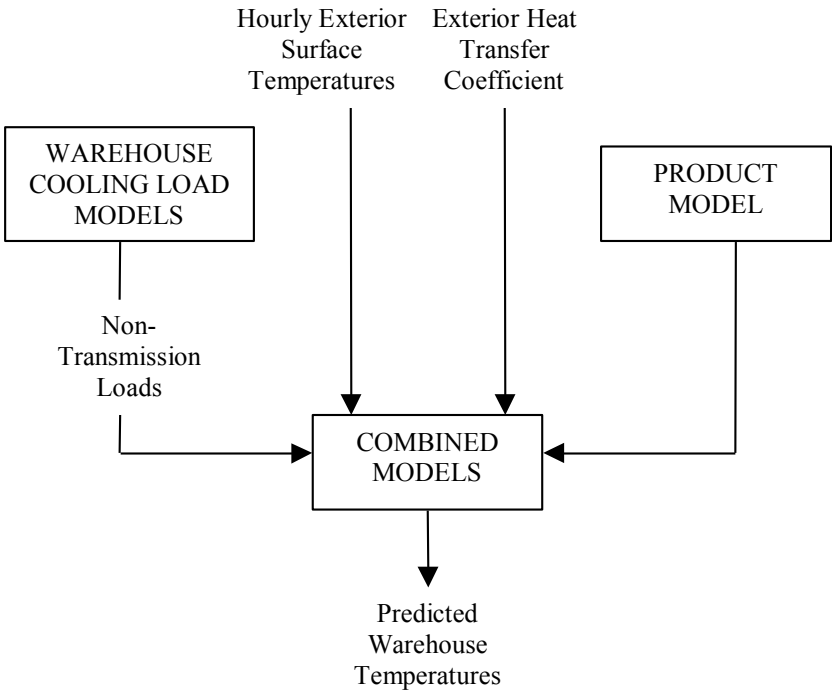

Separate models were created for warehouses “A & B”, “C”, and “D” using this process. Individual models were once again necessary not only due to differences in warehouse construction, but also due to differences in the product-to-air volume ratios in each warehouse. For example, the model created for warehouses “A” & “B” needed only a single layer of insulation for the walls and roof, while warehouse “C” required three layers (concrete, insulation, then concrete) for its walls. The roof of warehouse “D” needed layers comprised of steel and insulation. Also, the product pallets in warehouse “D” are stacked on individual metal shelves. This spaced arrangement of product results in less product volume per unit of storage space than in warehouses “A”, “B”, or “C”. To accommodate this change, the size of the product “block” at the center of the combined warehouse FEHT model was reduced until the ratio of the product volume to air volume matched the actual warehouse. Each model was created to emulate the existent warehouse as closely as possible. With all the necessary inputs in place, each model was run for a 14-hour period (8 AM to 10 PM, corresponding to the on-peak period at this facility) using the outdoor design conditions.

4.2. Results

The results were calculated for each warehouse, and are shown in Figures 4.3, 4.4, and 4.5. Each plot illustrates the temperature rise over the 14-hour on-peak window during a design day. Three points within the models are shown: the air temperature, a corner of the product block, and the center of the product block. Assuming the initial temperature within the warehouse is –5°F, the model predicts a final air temperature

above 0°F, the acceptable maximum temperature limit for long-term storage of frozen vegetables. In warehouses "A", "B", and "C", the product corners also rise above zero, indicating that these warehouses would need to be pre-cooled (below –5°F) in order to keep product temperatures below zero. Only warehouse "D" stays below the limit, even on the most exposed areas (corners). Differences in the model for warehouse "D", including the construction of the roof and the increased volume of air, contribute to this result. The centers of the product consistently stay at -5°F, confirming the prediction of the original product model in which the center of the stack of product was unaffected by environmental changes.

Figure 4.3. Predicted Temperature Rise: Warehouses "A" & "B"

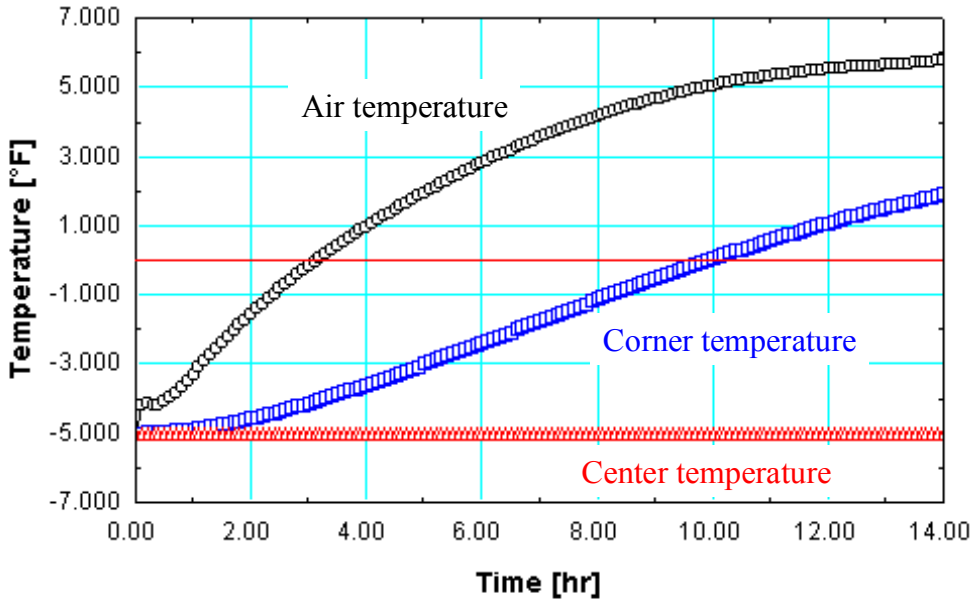

Figure 4.4. Predicted Temperature Rise: Warehouse "C"

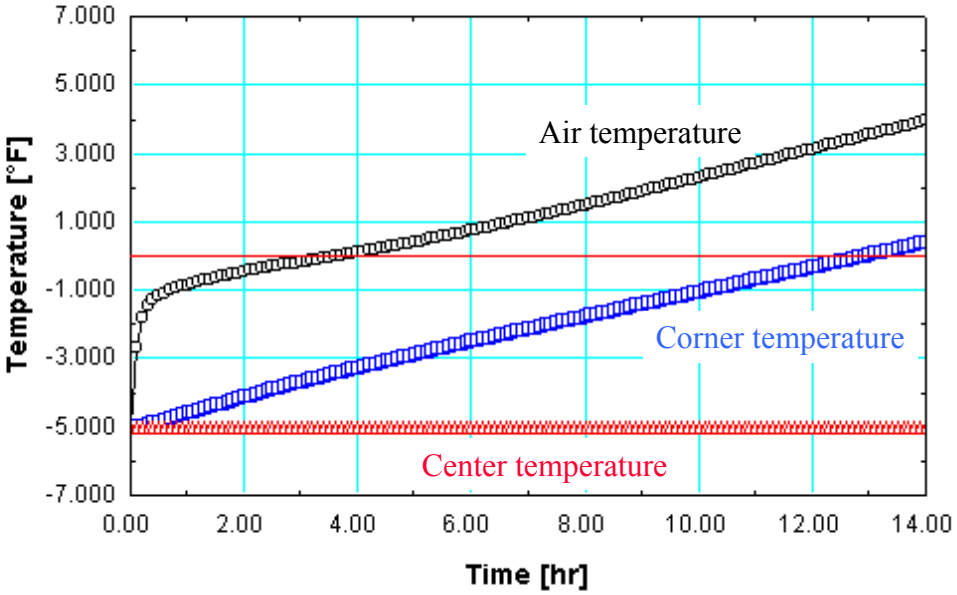

Figure 4.5. Predicted Temperature Rise: Warehouse "D"

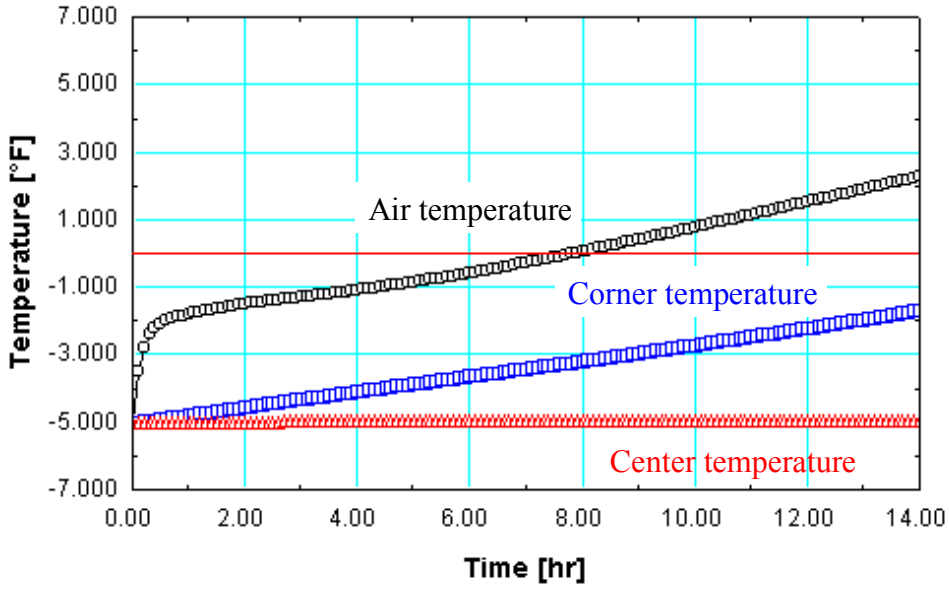

The results obtained from the combined model mark the completion of the initial development of a computer model of the warehouses. The next section discusses the experimental validation of the model, the final phase in its creation.

4.3. Experimental Validation

The purpose of recording actual experimental data from the warehouses is to verify the temperature rise predicted by the computer modeling, as well as to validate individual components used within the model. These include model inputs such as infiltration rates and interior convection coefficients. The experimental validation phase of the project began in April 1998. Experimental data, in the form of temperatures, air velocity measurements, and air infiltration rates, were taken at the facility. Data were recorded on three separate occasions: April 19, June 26, and August 25, 1998. The refrigeration equipment was shut down for a four-hour period, during which temperature measurements were recorded at short time intervals. These measurements were made at several locations throughout each warehouse, and a recorder was placed both near the ceiling and near the floor at each location. Air velocity measurements within the warehouses were used to substantiate the values used in the calculation of the heat transfer coefficient on the surface of the product packaging described in chapter 2. Recording air velocities at regular height intervals in an open doorway also validated infiltration rates estimated during the calculation of the cooling load. To monitor baseline operating conditions in the warehouses, temperature recorders were left at the facility for extended periods in April and July.

Measurements from the four-hour "floating" tests were compared with the predictions of the combined model obtained by inputting matching weather conditions. The comparison indicated that minor alterations to the calculated cooling load were needed. Corrections, including adjustments to the heat gained from lights and people, were made. Heat gains from the lights were reduced 20% in "A", "B", and "D" to account for actual intermittent use of warehouse lights, which are motion-activated. Other reductions were more arbitrary in nature and varied by warehouse model; all changes were made to adjust the load to cause a predicted temperature rise that matched the experimental data. For example, infiltration loads were increased by 25% to 50% depending on the overall adjustment needed. Heat gains from forklifts (which can change hourly) and entering product (which can change hourly and seasonally) were also increased or decreased by 10 to 20 %, again depending on the individual adjustments needed for each model. Total corrections to the refrigeration load ranged from 3 to 11% of the entire load. With these modifications in place, the models are now used to confidently predict the performance of the warehouses under any specified weather conditions. Figures 4.3, 4.4, and 4.5 shown in the previous section were calculated with the corrected models.

In addition to providing validation for the computer models, the experimental data produced two other pieces of valuable information. First, recording temperatures in both high and low positions in the warehouses showed that the warehouse air stratifies as it warms. Figure 4.6 is provided as an example of this phenomenon. The sensor positioned in the top of the warehouse warms up more quickly than those placed directly below.

This trend was recorded throughout all of the warehouses. Second, temperature measurements obtained during the extended baseline monitoring in April and July indicated that warehouses "A" & "B" were not holding at the desired set point of –5°F. These two warehouses have significantly less refrigeration capacity per cooling load than both "C" and "D". Calculations show that a minimum of 25 additional tons of capacity is needed to maintain the air at –5°F under design conditions. Figure 4.7 shows temperatures in warehouses "A" and "B" for the month of July. The uncertainty of the temperature measurement devices is +/- 0.6°F. A seemingly unrelated but conspicuous spike in the temperature of the warehouse occurs near July 2, 1998. Attempts to investigate the cause of the increase were unsuccessful because daily warehouse logs for that time, a holiday weekend, could not be located.

Figure 4.6. Experimental Data: Warehouse "C", August 25, 1998

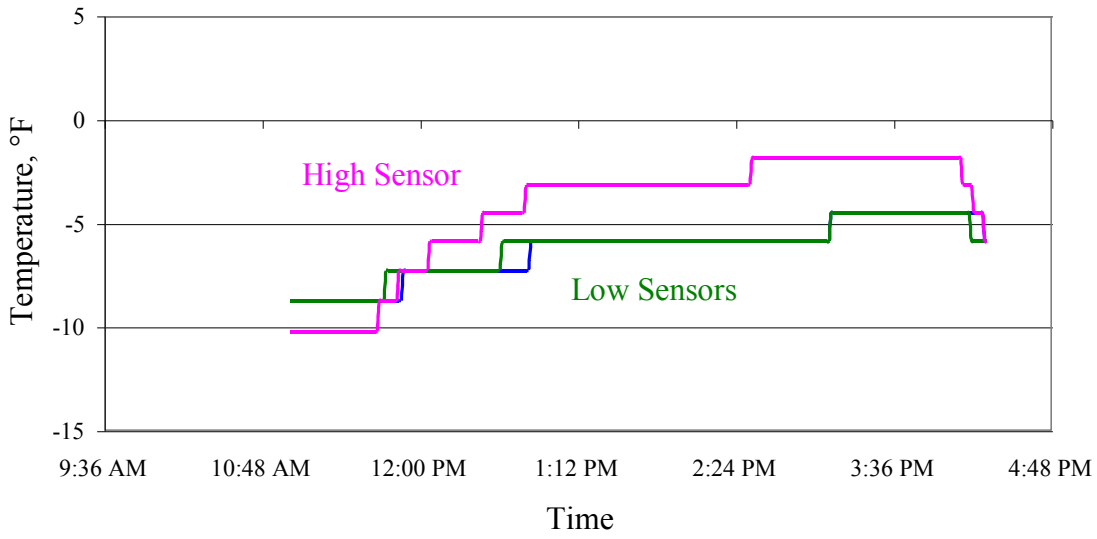

Figure 4.7. Warehouse "A" Baseline Temperatures, Month of July 1998

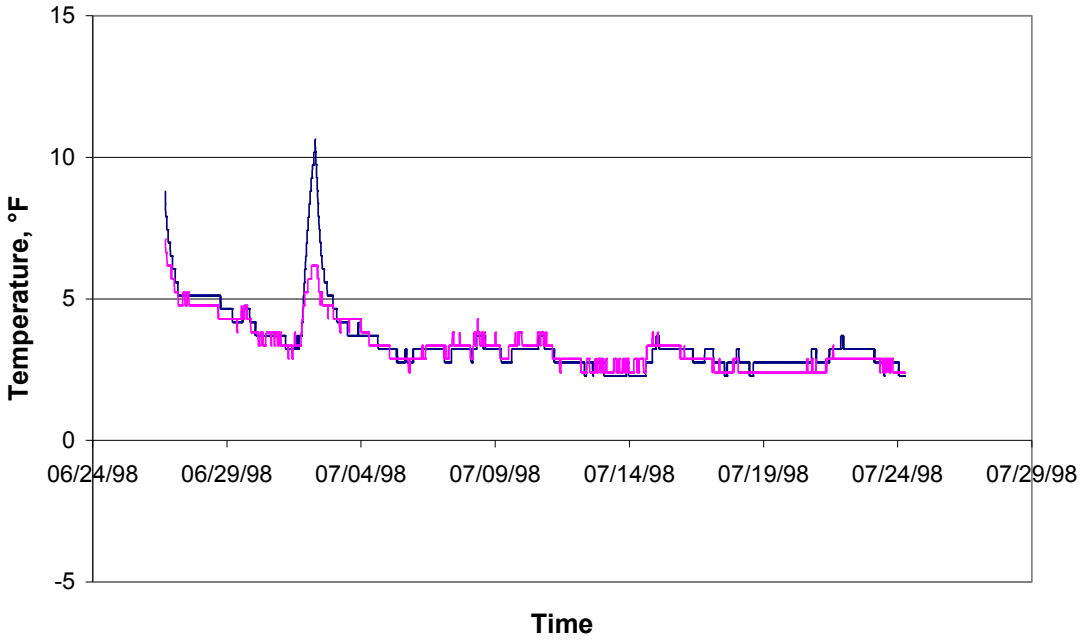

Experimental validation is necessary in order to adjust the output of the model as a whole and guarantee its agreement with actual warehouse performance. Equally valuable is an understanding of what effect each of the model's inputs has on the overall model behavior. The next section, Sensitivity Analysis, describes the process used to examine the sensitivity of the models to individual parameters.

4.4. Sensitivity Analysis

Each model's sensitivity to individual inputs, including the three thermal properties of frozen vegetables discussed in section 2.4.1, the heat transfer coefficient on the interior of the warehouse, and the heat transfer coefficient on the exterior of the warehouse are analyzed according to the following procedure. First, each model is run

using the baseline values for all inputs and design conditions. The temperature rise occurring after 14 hours is recorded for each location in the model (air, product corner, and product center). One by one, the magnitude of the model inputs are varied first by + 50%, then –50%, and the corresponding 14-hour temperature rise is again recorded in each case. The comparison between the temperature rise occurring under baseline conditions and the temperature rise caused by the change in one variable shows the effect of that particular variable on the whole model. As an example, Figure 4.8 shows the temperature rise in warehouse "C" after 14 hours varying the density of the stored product. As expected, there was a 0°F rise in temperature at the center of the product using the "normal" (baseline) value for density. Changing the value of the density had no effect at the center of the product. However, the corner temperature rose an additional 2°F when the density was decreased by 50%.

Figure 4.8. Warehouse "C": Sensitivity to Product Density, Design Conditions

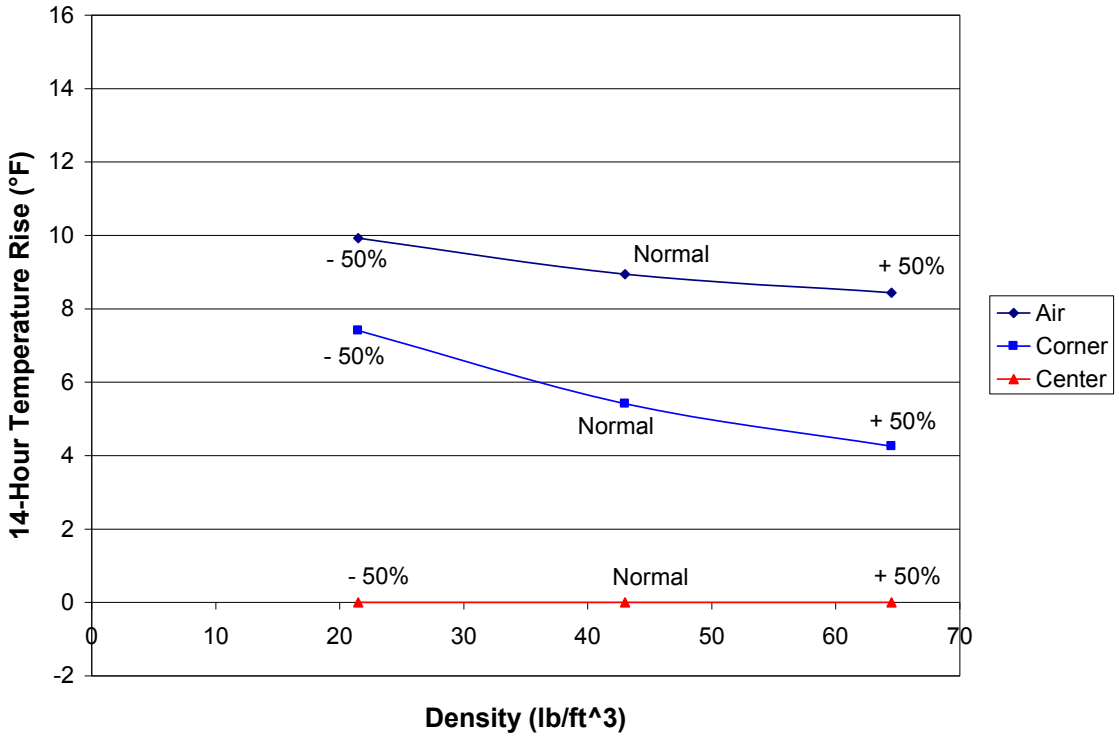

Table 4.1 is included as a summary of the entire sensitivity analysis. The values in the table represent the increase or decrease of the 14-hour temperature rise (in °F) as compared to the results obtained using the "normal" model inputs. Large values indicate that the model is very sensitive to that individual input. Decreasing the interior heat transfer coefficient by 50% produced notable increases in the air temperature in all three models. Conversely, neither increasing nor decreasing the thermal conductivity of the product had any significant effect in any model. These results indicate which model inputs are the most crucial to the calculated results, as well as how changes in the actual storage environment and product characteristics are likely to affect the thermal performance of the warehouse.

Table 4.1. Summary of Warehouse Model Sensitivity Analysis

		Warehouse "A" & "B"			Warehouse "C"			Warehouse "D"		
		Air	Corner	Center	Air	Corner	Center	Air	Corner	Center
Density	+ 50%	-0.97	-1.66	0.00	-0.50	-1.16	0.00	-0.36	-0.84	-0.01
	- 50%	1.99	3.13	0.00	0.98	1.99	0.00	0.73	1.69	-0.01
Thermal Conductivity	+ 50%	-0.27	-0.38	0.00	-0.14	-0.28	0.00	-0.08	-0.11	-0.01
	- 50%	0.33	0.46	0.00	0.18	0.34	0.00	0.09	0.13	0.02
Specific Heat	+ 50%	-0.97	-1.66	0.00	-0.50	-1.16	0.00	-0.36	-0.84	-0.01
	- 50%	1.99	3.13	0.00	0.98	1.99	0.00	0.73	1.69	-0.01
Interior Heat Transfer Coefficient	+ 50%	-1.63	-0.12	0.00	-1.23	-0.03	0.00	-0.96	0.16	0.00
	- 50%	4.77	-0.09	0.00	3.60	0.00	0.00	2.79	-0.24	-0.01
Exterior Heat Transfer Coefficient	+ 50%	0.01	0.01	0.00	0.07	0.03	0.00	0.07	0.02	0.00
	- 50%	-0.04	-0.04	0.00	-0.17	-0.08	0.00	-0.19	-0.06	0.00

With a reliable computer model, the next step in the project is the analysis of possible demand shifting strategies. By inputting monthly weather data, the model can be used to predict the total annual load for the warehouses. The following chapter discusses three possible strategies, predicted warehouse temperatures for the strategies, and the economic impact expected from their implementation.

Chapter 5

DEMAND SHIFTING STRATEGIES

5.1. Full Demand Shifting

Three demand shifting options were analyzed for possible implementation at the facility. The first option, full demand shifting, requires a complete shutdown of all refrigeration equipment during the specified 14-hour on-peak time window. This option offers the greatest demand reduction leading to the most on-peak energy savings, but requires the greatest installed refrigeration capacity. In this case, the refrigeration system must be able to eliminate all heat gained (over 24 hours) in only the 10 hours available during the off-peak window. Only two ("C" & "D") of the four warehouses currently have enough installed refrigeration evaporator capacity to implement this option. Figures 5.1, 5.2, and 5.3 show the calculated temperature variations inside the four warehouses using full demand shifting. The plots display results for 0 to 72 hours, corresponding to three consecutive design days. In all situations, the product temperature stays below the 0°F limit. Once again, the center of the product arrangement stays at a constant –5°F. The corner of the product, which is expected to undergo the largest temperature fluctuations, varies between approximately –12.5°F and –2.5°F in the worst case (Figure 5.1). In all warehouses, the average temperature on the corner of the product is below –5°F, which is beneficial to the quality of the product. Because the model was run for

only three consecutive days, the temperature on the corners of the product does not have time to begin affecting the product near the center of the stacks. If the model were allowed to run for many days or even months, the center temperature would eventually begin to approach the average corner temperature. However, the actual occurrence of more than three consecutive design days is small, so results for longer time periods would become unrealistic.

Figure 5.1. Warehouses "A" & "B": Full Shifting Strategy, Three Design Days

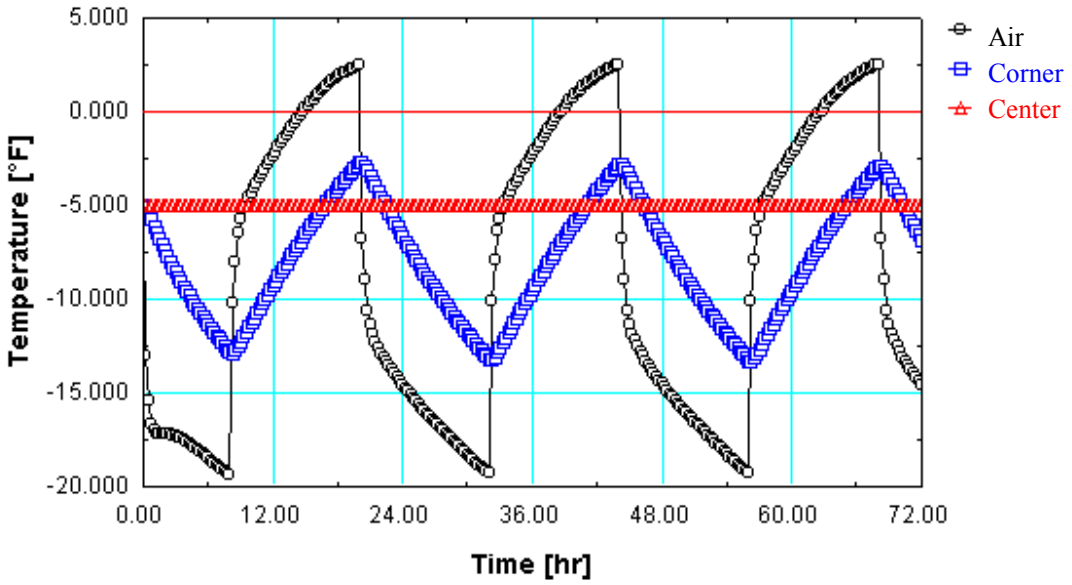

Figure 5.2. Warehouse "C": Full Shifting Strategy, Three Design Days

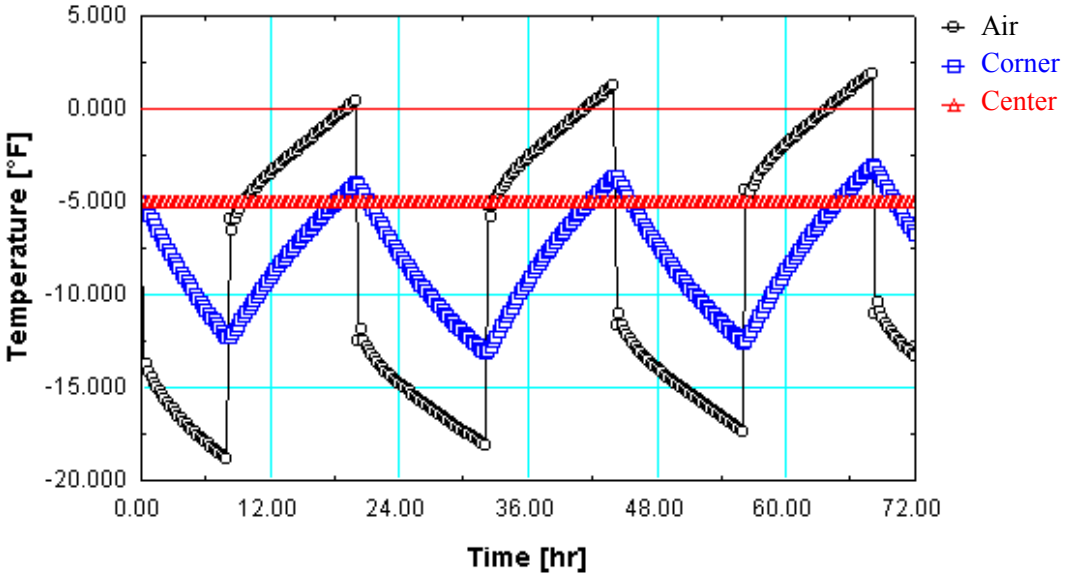

Figure 5.3. Warehouse "D": Full Shifting Strategy, Three Design Days

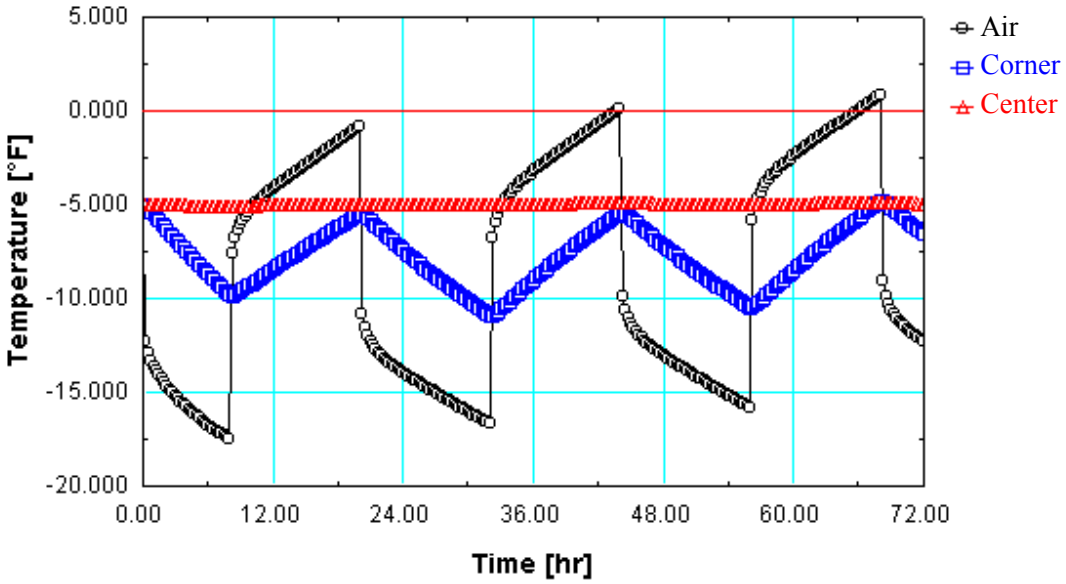

The differences in the temperature response between the three models are due to the variances in the models examined in chapter 4. The total refrigeration load in

warehouses “A” & “B” is the largest of the three, and the load peaks during the middle of the on-peak period. This causes a larger rise in temperature during “floating” than occurs in warehouses “C” or “D”. The concrete construction in warehouses “C” and “D” shifts the peak load later into the evening, so the bulk of the load occurs during off-peak. Differences between warehouses “C” and “D” are due to the smaller product-to-air volume ratio in warehouse “D” and the construction differences in the roof, as discussed in sections 4.1 and 4.2.

One additional advantage of the full demand shifting strategy is its ease of operation. To implement this strategy, warehouse operators must simply shut down their refrigeration system(s) during the on-peak time window, then restart during the off-peak period. No further controls are necessary. One possible exception involves cycling the evaporator fans to reduce air stratification, which is not required but certainly advisable. This option is discussed further in section 6.2.

5.2. Load Leveling

A second option, load leveling, meets the load in each warehouse by running the equipment at a constant level throughout the 24-hour period. In effect, this option slightly over-cools each warehouse at night and slightly under-cools it during the day as the warehouses’ loads vary. This operating strategy offers the least savings of the three options, but it requires the least amount of installed equipment capacity. Using the model previously developed, the temperatures of the air, product corner, and product center of each warehouse under this operating strategy are shown in Figures 5.4, 5.5, and 5.6.

Figure 5.4. Warehouses "A" & "B": Load Leveling Strategy, Three Design Days

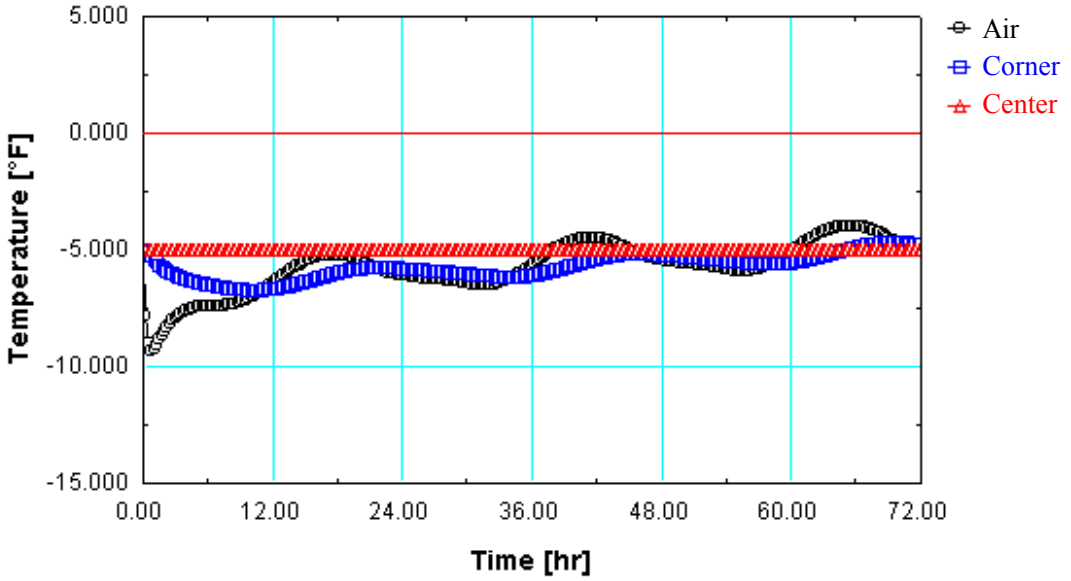

Figure 5.5. Warehouse "C": Load Leveling Strategy, Three Design Days

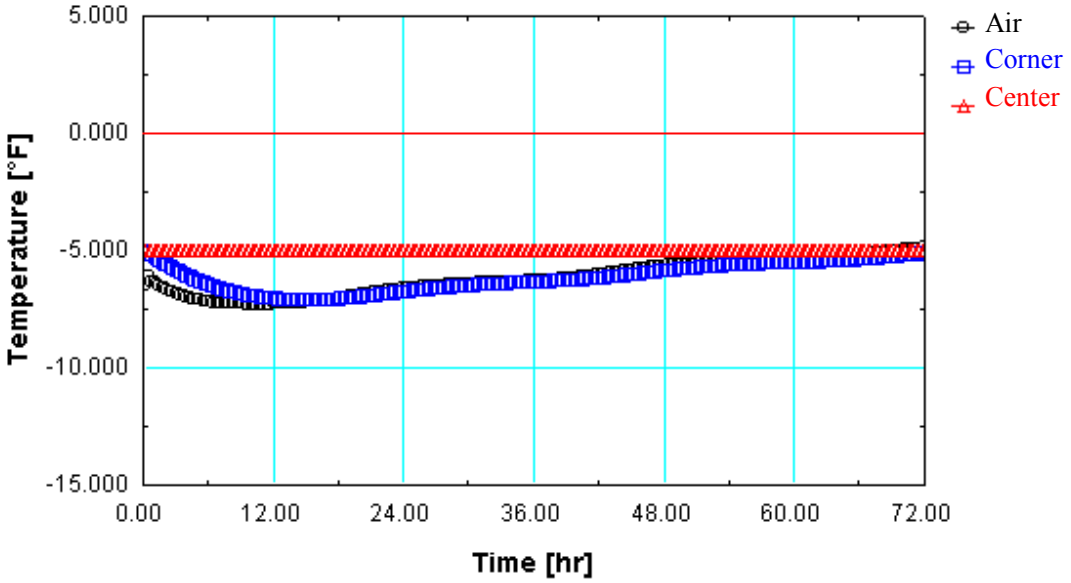

Figure 5.6. Warehouse "D": Load Leveling Strategy, Three Design Days

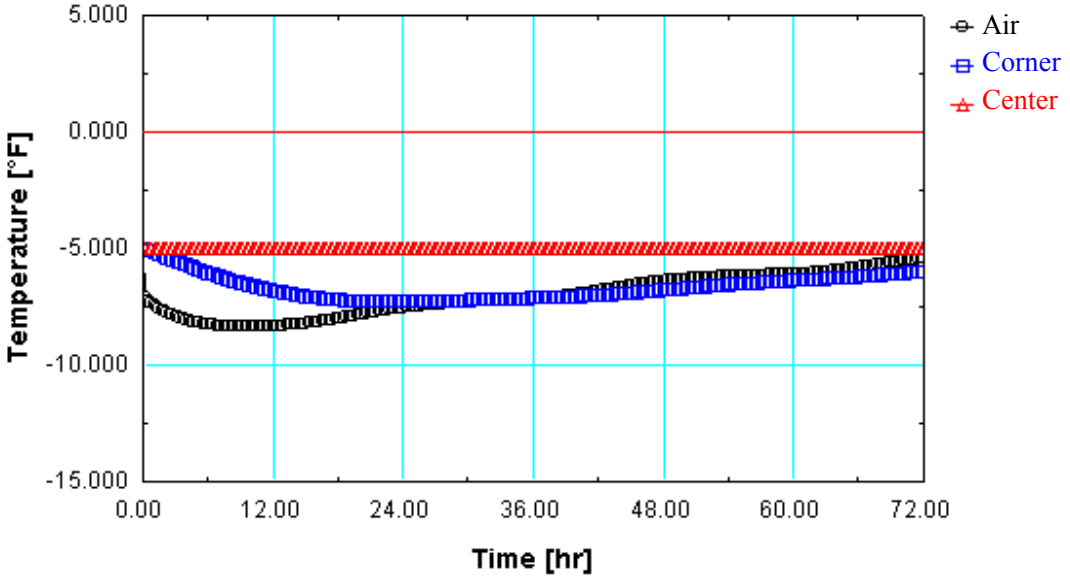

The figures indicate less temperature variation using this strategy than with the full shifting option. This, along with reduced refrigeration capacity requirements, is an advantage of this strategy. However, relatively little is saved in cost or energy use. The economics are described in greater detail in section 5.4.

5.3. Combination

The third option is a combination of the first two. The refrigeration runs at one level during the day and a higher level at night. This strategy requires less total capacity than full demand shifting, but offers more savings than load leveling. The additional savings are gained during colder months, when the cooling load is lower. Depending on the capacity of the warehouse, full demand shifting may be possible during the winter

months under this third alternative. Figure 5.7 is included as an example of the temperature response of a warehouse operating under this type of strategy. Because both warehouses "C" and "D" currently have enough installed capacity to use full demand shifting all year, only warehouses "A" & "B" show temperature variations different than those included in section 5.1. Figure 5.7 shows the response of warehouses "A" & "B" during three "typical" days in the month of April. Assuming that the additional 25 tons (88 kW) of refrigeration capacity discussed in section 4.3 are added, warehouses "A" & "B" would then have only enough installed capacity to just meet the design load. Under design conditions, the equipment would have to run at 100% of capacity both on and off peak. The month of April was selected to show an example of the combined option. The figure shows moderate temperature fluctuations induced by the reduced level of refrigeration during the on-peak time window.

Figure 5.7. Warehouses "A" & "B": Combined Strategy, Three Days in April

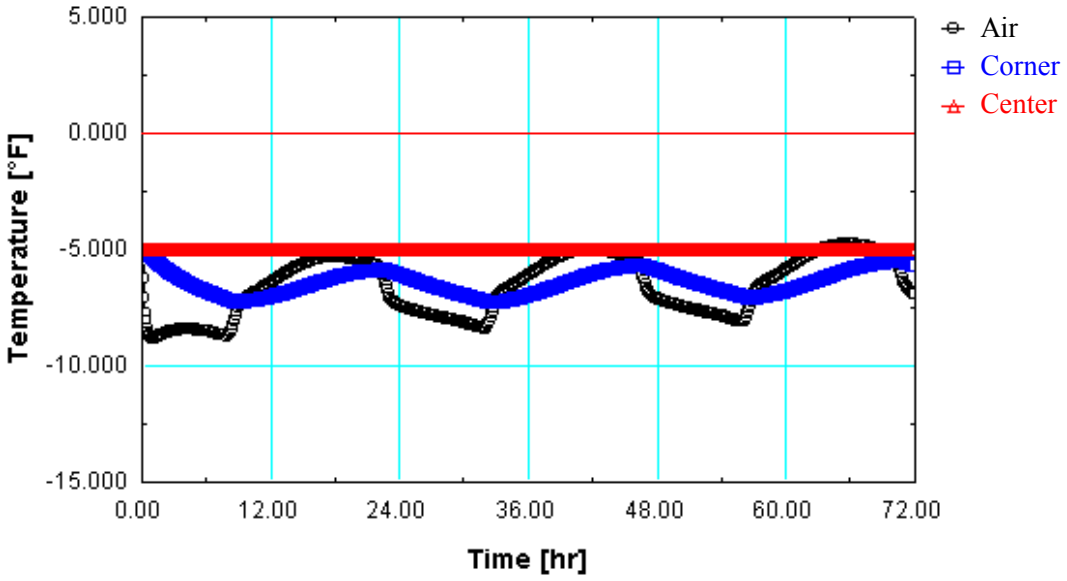

While this strategy offers significant advantages in terms of capacity requirements and cost savings, its major drawback is in implementation. In order to determine what levels to run the equipment at during the two rate periods, the warehouse operators must be able to predict the daily load of each warehouse at least one day in advance. Theoretical predictions of the average or typical load can be made easily, but actual daily variations can be significant. For example, a warehouse operator must decide a day in advance what the next day's load will be. The operator logically chooses to operate the equipment at full capacity during the off-peak period, but then must choose what lower level to operate at during on-peak hours. Based on the assumption of what the day's load will be, an on-peak level is selected. Ideally, the amount of heat removed by the equipment during off-peak hours plus the amount removed during the on-peak period equals the total load. However, if the on-peak level selected was too small, not all heat gain will be removed, and the warehouse temperatures will rise. If the level selected is too large, the warehouse will be overcooled. While this is not a problem from a product quality perspective, the warehouses will be using more energy than necessary, which reduces overall savings. Assuming the operator will always choose the on-peak level conservatively, the annual savings offered by this option could be reduced significantly over the theoretical, "perfect operation", savings to be discussed in section 5.4.

5.4. Economic Analysis

In order to determine which of the previous three strategies is most desirable, an economic analysis of each option is necessary. The first step in this process is to analyze

the default option: normal operation. By applying an entire year's weather data to the warehouse models, the total annual load in each of the warehouses is calculated. Next, the total annual cost of operating the warehouses under normal conditions is calculated knowing the amount of power the refrigeration system uses per unit of cooling. For example, if the cooling load is 200 tons and the system performance is 2 kW per ton of cooling, then the system uses 400 kW of power to meet the cooling load. The system performance is dependent on the outside air wet-bulb temperature, so its value changes hourly throughout the year. Additional electrical loads attributable to the warehouses must also be added, such as lights and evaporator fans. In effect, these items "cost double" to operate, since the initial electrical power must be purchased, then the heat they generate must be removed by the refrigeration system. Once the total electrical load is calculated, the annual cost for normal operation is computed using the utility rate structure. In this case, all weekends, holidays, and weeknights (between 10 PM and the following 8 AM) are considered off-peak times. As a means of reducing the number of calculations, weather conditions for the "typical" day of each month were applied to the warehouse models in place of annual weather data. By assuming the "typical" weather conditions are applicable to every day in the month, the calculations were reduced from all 365 days of the year to only 12 days, each representing one month. The outdoor wet-bulb temperatures for each "typical" day were also used to generate the refrigeration system performance values. The error introduced by using this calculation method is very small. In the test case, the load obtained using the "typical" weather data for a July day produced a 0.07% error when compared with the average load obtained by using

hourly weather data for the entire month of July (744 hours). The only difference between these two methods lies in the transmission portion of the refrigeration load. Only the transmission load is contingent upon the weather; the load is linearly dependent on the temperature difference between the inside and outside of the warehouse. Since the hourly temperatures for the "typical" day of July are the average of the hourly temperatures for all 31 days, then logic dictates that the load calculated using the average temperatures is equal to the averaged load calculated using the individual temperatures. The 0.07% difference is small enough to be attributed to rounding of decimals in the calculations. Using the "typical" day method saved significant computational effort. Instead of completing the calculations for every hour of a month, then averaging the result at the end, the weather data was averaged first and used in calculations for only 24 hours.

The next step in the economic analysis is to determine the costs associated with each of the three operating strategies, then figure the savings over normal operation in each case. The method used to calculate the cost of normal operation is also used for each demand shifting option, so differences in the total costs are due to the distribution of the loads during the on and off-peak times. The results of the investigation were organized into a spreadsheet for simple comparison and easy alteration. Under normal operating conditions, the annual operating cost of all warehouses is nearly $155,000. Using full demand shifting, this total falls to around $73,000, a 53% savings. However, as mentioned previously, additional capacity must be added at this facility in order to implement this option. Assuming that additional capacity has an associated capital cost

of $1,000 per ton, full demand shifting will require an investment of about $130,000. Combined with the savings this method would generate, the simple return-on-investment is 62%. With load leveling, only about $1,000 is saved. Using the third option, slightly more than $58,000 is saved and no additional capacity is required. As mentioned in the last section, this savings is realized when the night and day levels are chosen perfectly. In real operation, the savings will likely be smaller. All of the above estimates are based on the assumption that the additional 25 tons of capacity required for operation in warehouses "A" and "B" have been added. Therefore, to implement full demand shifting, the total expenditure based on current operating conditions is $155,000.

The economic projections presented here are dependent on a variety of factors. For example, if the estimated cost of adding additional refrigeration capacity is more than $1,000 per ton, then the cost of upgrading the system for demand shifting will be greater than what is shown. The operating parameters of the refrigeration system, including the minimum allowable condenser temperature and saturated suction temperature, also greatly influence the cost predictions. The values shown here are based on the information supplied by the warehouse operators. To observe the effects of altering these parameters, each component was built into the spreadsheet created for calculating the annual load and costs. In this way, the item can be changed easily and its effect on the bottom line seen immediately. By decreasing the condenser temperature by 5°F, for example, the normal annual operating cost drops approximately $4,000. The spreadsheet allows the user to change utility rates, refrigeration system parameters, investment costs, and select between a 14-hour and 12-hour on-peak period. An additional feature allows

the user to specify how many minutes per hour, if any, to cycle evaporator fans. Again, each of these inputs alters the final savings estimates for each operating strategy. The spreadsheet was designed for use by warehouse operators, as well as utility employees, in making informed operating decisions.

Completion of the development and analysis of three viable demand shifting strategies marks the conclusion of this investigation. Due to the lack of evaporator capacity in two of the four warehouses at this facility, implementation of a demand shifting strategy was not attempted. In chapter six, the findings of this study are summarized and supplemented with recommendations for future work.

Chapter 6

SUMMARY AND RECOMMENDATIONS

6.1. Summary

This study was undertaken to test the feasibility of using the thermal mass of products stored in a refrigerated warehouse to shift on-peak electrical demand to off-peak. A frozen vegetable processing and warehousing facility in southeastern Wisconsin was chosen as the test subject for the project. By gathering information about the properties of the products in storage, as well as the characteristics of the warehouse structures, computer models of the thermal performance of the warehouses at the facility were created. The annual load and resulting electrical costs of the warehouses were calculated by applying yearly weather data to the models and analyzing the results. Three possible demand shifting strategies were studied using the output from the models. Full demand shifting could be implemented at this facility, but additional refrigeration capacity must be added. This operating strategy will save approximately $82,000 (53%) over normal operation and would be simple to implement. Another worthwhile strategy combines the full shifting and load leveling techniques, which will save $58,000 (37%) without the need for more capacity. However, this technique requires a comparatively sophisticated control strategy for actual implementation, and in reality would offer lower savings than indicated. Load leveling alone only saves about $1,000 annually. The

largest product temperature fluctuations, from –12.5°F to –2.5°F, occur using the full demand shifting technique. This range of variation is not expected to have any detrimental effects on the quality of the products in storage.

6.2. Recommendations

Decisions regarding which operating technique to implement are left to the utility and warehouse owners. In any event, an additional 25 tons of capacity is necessary in warehouses "A" and "B" simply to meet the existing load, and should be installed as soon as reasonably possible.

Several factors concerning the operation of the refrigeration equipment affect the total load and energy costs. Among these factors are the minimum allowable condenser temperature, saturated suction temperature, and optional fan cycling during on-peak operation. In general, the highest possible suction temperature and the lowest possible condenser temperature are desirable for optimal system performance. Based on the experimental data recorded at the site, periodic fan cycling in each warehouse is recommended. Cycling the evaporator fans for a few minutes each hour does not add any significant cost, and will diminish the effects of stratification. In order to control the cycling of fans, routinely monitor warehouse and refrigerant temperatures, and efficiently manage any operating strategy, the installation of a control system is also recommended. Should more utilities begin to adopt "real time" pricing, under which electricity prices are determined only a day or even a few hours in advance, a flexible and responsive control system would be a wise investment.

A final possibility for consideration is a 12-hour on-peak rate plan. Assuming this warehouse facility is free to choose between the 14-hour and 12-hour plans, the 12-hour plan offers the advantage of requiring significantly less installed refrigeration capacity. The overall annual cost is slightly higher than with the 14-hour plan due to higher rates, but the difference in savings is relatively small (about $4,000). Under the 12-hour plan, $94,000 in capital costs is required for full demand shifting, which corresponds to a simple return-on-investment of approximately 83%.

All of the aforementioned possibilities and recommendations are built into the interactive spreadsheet, so that their effects can be easily observed in the final analysis. The spreadsheet is designed to be user-friendly, and will show the hourly load and annual economic analysis for each warehouse at the site.

6.3. Future Research

Future work in several areas would greatly add to the general applicability of this research. First and perhaps foremost, the entire study should be repeated at a facility that stores products at higher temperatures. Before the results of this study can be applied to any storage facility, the effect of this type of operating strategy on other types of products must be known. In conjunction, study of another type of refrigerated storage facility will aid in the development of general guidelines. A concise set of guidelines for what types of facilities should consider demand shifting, as well as what products (if any) should not be subjected to this type of storage, would be highly beneficial to both the refrigerated

warehousing industry and electric utilities desiring to initiate demand reduction programs.

The effect of weekly storage cycles was not studied during the course of this project, and its impact may merit investigation. The model developed for this project was run for a maximum of three design days. However, a real warehouse operation would include two full days of off-peak hours every weekend. These days could be used to provide additional pre-cooling and would effect the temperature response of the warehouses throughout the remainder of the week. Additional modeling of this effect in the form of weekly or monthly cycling is recommended.

While the results of an extensive literature search gave no indication that temperature cycling in the range expected using demand shifting would harm frozen vegetables, a direct investigation is advisable. A controlled study subjecting the product to the same conditions as would occur in the warehouse setting would provide direct evidence. If demand shifting indeed proves harmless to product quality, the fears of warehouse operators would be greatly allayed, fostering greater acceptance of this technique.

Appendix A

Contents

Pages 68-70 are placeholders for the printed version of EES model file “Heat.ees”. This data file is available in the supplemental CD or by contacting the author.

Pages 68-70 are placeholders for the printed version of EES model file “Heat.ees”. This data file is available in the supplemental CD or by contacting the author.

Pages 68-70 are placeholders for the printed version of EES model file “Heat.ees”. This data file is available in the supplemental CD or by contacting the author.

Appendix B

Contents

1. EES program calculating exterior surface temperatures (sol-air)
2. EES program calculating the transmission load through the floor
3. EES program calculating the transmission load through the walls and roof of warehouses “A” & “B”
4. EES program calculating the transmission load through the walls of warehouses “C” and “D”
5. EES program calculating the transmission load through the roof of warehouse “C”
6. EES program calculating the transmission load through the roof of warehouse “D”

Pages 72-77 are placeholders for the printed version of EES model file "MonthlyTemps.ees". This data file is available in the supplemental CD or by contacting the author.

Pages 72-77 are placeholders for the printed version of EES model file "MonthlyTemps.ees". This data file is available in the supplemental CD or by contacting the author.

Pages 72-77 are placeholders for the printed version of EES model file "MonthlyTemps.ees". This data file is available in the supplemental CD or by contacting the author.

Pages 72-77 are placeholders for the printed version of EES model file "MonthlyTemps.ees". This data file is available in the supplemental CD or by contacting the author.

Pages 72-77 are placeholders for the printed version of EES model file "MonthlyTemps.ees". This data file is available in the supplemental CD or by contacting the author.

Pages 72-77 are placeholders for the printed version of EES model file "MonthlyTemps.ees". This data file is available in the supplemental CD or by contacting the author.

Pages 78-79 are placeholders for the printed version of EES model file “floorload.ees”. This data file is available in the supplemental CD or by contacting the author.

Pages 78-79 are placeholders for the printed version of EES model file “floorload.ees”.

This data file is available in the supplemental CD or by contacting the author.

Pages 80-86 are placeholders for the printed version of EES model file “transA&B.ees”. This data file is available in the supplemental CD or by contacting the author.

Pages 80-86 are placeholders for the printed version of EES model file “transA&B.ees”.

This data file is available in the supplemental CD or by contacting the author.

Pages 80-86 are placeholders for the printed version of EES model file “transA&B.ees”. This data file is available in the supplemental CD or by contacting the author.

Pages 80-86 are placeholders for the printed version of EES model file “transA&B.ees”.

This data file is available in the supplemental CD or by contacting the author.

Pages 80-86 are placeholders for the printed version of EES model file “transA&B.ees”. This data file is available in the supplemental CD or by contacting the author.

Pages 80-86 are placeholders for the printed version of EES model file “transA&B.ees”.

This data file is available in the supplemental CD or by contacting the author.

Pages 80-86 are placeholders for the printed version of EES model file “transA&B.ees”. This data file is available in the supplemental CD or by contacting the author.

Pages 87-93 are placeholders for the printed version of EES model file “transC&D.ees”.

This data file is available in the supplemental CD or by contacting the author.

Pages 87-93 are placeholders for the printed version of EES model file “transC&D.ees”. This data file is available in the supplemental CD or by contacting the author.

Pages 87-93 are placeholders for the printed version of EES model file “transC&D.ees”.

This data file is available in the supplemental CD or by contacting the author.

Pages 87-93 are placeholders for the printed version of EES model file “transC&D.ees”. This data file is available in the supplemental CD or by contacting the author.

Pages 87-93 are placeholders for the printed version of EES model file “transC&D.ees”.

This data file is available in the supplemental CD or by contacting the author.

Pages 87-93 are placeholders for the printed version of EES model file “transC&D.ees”. This data file is available in the supplemental CD or by contacting the author.

Pages 87-93 are placeholders for the printed version of EES model file “transC&D.ees”.

This data file is available in the supplemental CD or by contacting the author.

Pages 94-99 are placeholders for the printed version of EES model file "roofloadC&D.ees". This data file is available in the supplemental CD or by contacting the author.

Pages 94-99 are placeholders for the printed version of EES model file "roofloadC&D.ees". This data file is available in the supplemental CD or by contacting the author.

Pages 94-99 are placeholders for the printed version of EES model file "roofloadC&D.ees". This data file is available in the supplemental CD or by contacting the author.

Pages 94-99 are placeholders for the printed version of EES model file "roofloadC&D.ees". This data file is available in the supplemental CD or by contacting the author.

Pages 94-99 are placeholders for the printed version of EES model file "roofloadC&D.ees". This data file is available in the supplemental CD or by contacting the author.

Pages 94-99 are placeholders for the printed version of EES model file "roofloadC&D.ees". This data file is available in the supplemental CD or by contacting the author.

This page intentionally left blank.

Appendix C

Contents

Pages 102-105 are placeholders for the printed version of EES model file "DeanInfiltration.ees". This data file is available in the supplemental CD or by contacting the author.

Pages 102-105 are placeholders for the printed version of EES model file "DeanInfiltration.ees". This data file is available in the supplemental CD or by contacting the author.

Pages 102-105 are placeholders for the printed version of EES model file "DeanInfiltration.ees". This data file is available in the supplemental CD or by contacting the author.

Pages 102-105 are placeholders for the printed version of EES model file "DeanInfiltration.ees". This data file is available in the supplemental CD or by contacting the author.

This page intentionally left blank.

Appendix D

Contents

Pages 108-111 are placeholders for the printed version of EES model file "kWperton.ees". This data file is available in the supplemental CD or by contacting the author.

Pages 108-111 are placeholders for the printed version of EES model file "kWperton.ees". This data file is available in the supplemental CD or by contacting the author.

Pages 108-111 are placeholders for the printed version of EES model file "kWperton.ees". This data file is available in the supplemental CD or by contacting the author.

Pages 108-111 are placeholders for the printed version of EES model file "kWperton.ees". This data file is available in the supplemental CD or by contacting the author.

This page intentionally left blank.

References

American Society of Heating, Refrigerating, and Air-Conditioning Engineers (ASHRAE), 1993 ASHRAE Handbook – Fundamentals (I-P Edition), 1993.

American Society of Heating, Refrigerating, and Air-Conditioning Engineers (ASHRAE), 1997 ASHRAE Handbook – Fundamentals (I-P Edition), 1997.

American Society of Heating, Refrigerating, and Air-Conditioning Engineers (ASHRAE), 1990 ASHRAE Handbook – Refrigeration (I-P Edition), 1990.

American Society of Heating, Refrigerating, and Air-Conditioning Engineers (ASHRAE), 1994 ASHRAE Handbook – Refrigeration (I-P Edition), 1994.

Aparicio-Cuesta, M.P. and C. Garcia-Moreno, "Quality of Frozen Cauliflower during Storage" *Journal of Food Science,* 53.2 (1988): 491-493.

Ashby, B.H., A.H. Bennett, W.A. Bailey, W. Moleeratanond, and A. Kramer, "Energy Savings and Quality Deterioration from Holding Frozen Foods at Two Daily Temperature Levels" *Transactions of the ASAE,* (1979): 938-943.

Boggs, M.M., W.C. Dietrich, M. Nutting, R.L. Olson, F.E. Lindquist, G.S. Bohart, M.J. Neumann, and M.J. Morris, "Time-Temperature Tolerance of Frozen Foods XXI: Frozen Peas" *Food Technology,* 14 (1960): 181.

Cole, Ronald A., "Infiltration Load Calculations for Refrigerated Warehouses", *Heating/Piping/Air Conditioning*, April (1987): 45-54.

Dolan, K.D., R. Paul Singh, and D.R. Heldman "Prediction of Temperature in Frozen Foods Exposed to Solar Radiation" *Journal of Food Processing and Preservation,* 11 (1987): 135-158.

Duffie, J.A. and W.A. Beckman, Solar Engineering of Thermal Processes, 2nd Edition, John Wiley & Sons, Inc., 1991.

Gortner, W.A., F. Fenton, F.E. Volz, and E. Gleim, "Effect of Fluctuating Storage Temperatures on Quality of Frozen Foods" *Industrial Engineering and Chemistry,* 40 (8) (1948): 1423-1426.

Hustrulid, A. and J.D. Winter, "The Effect of Fluctuating Storage Temperature on Frozen Fruits and Vegetables" *Agricultural Engineering,* 24(12) (1943): 416.

Incropera, F.P. and D.P. DeWitt, Introduction to Heat Transfer, 2nd Edition, John Wiley & Sons, Inc., 1990.

International Institute of Refrigeration (IIR), Recommendations for the Processing and Handling of Frozen Foods, 3rd Edition, 1986.

Kamel, Basil, and Bashir Manji "Effect of Frozen Storage on Different Pizza Formulations" *Cereal Foods World,* 31.10 (1986): 751-755.

Klein, S.A. and F.L. Alvarado, "EES - Engineering Equation Solver," F-Chart Software, 1996.

Klein, S.A., W.A. Beckman, and G.E. Myers, "FEHT A Finite Element Analysis Program," F-Chart Software, 1995.

Krack Corporation, Refrigeration Load Estimating Manual, #RLE-593, 1992.

Kramer, Amihud, "Effects of Freezing and Frozen Storage on Nutrient Retention of Fruits and Vegetables" *Food Technology,* February (1979): 58-65.

Moleeratanond, W., Amihud Kramer, B.H. Ashby, W.A. Bailey, and A.H. Bennett, "Effect of Temperature Fluctuations on Energy Consumption and Quality Changes of Palletized Foods in Frozen Storage" *ASHRAE Transactions,* (1979): 56-65.

Rao, M.A. and S.S.H. Rizvi, Engineering Properties of Foods, 2nd Edition, Marcel Dekker, Inc., 1995.

Sastry, Sudhir K. and Arun Kilara, "Temperature Response of Frozen Peas to Di-Thermal Storage Regimes" *Journal of Food Science,* 48 (1983): 77-83.

Singh, R. Paul and C.Y. Wang, "Quality of Frozen Foods – A Review" *Journal of Food Process Engineering,* 1 (1977): 97-127.

Woodroof, J.G. and E. Shelor, "Effect of Freezing Storage on Strawberries, Blackberries, Raspberries, and Peaches" *Food Freezing,* February (1947): 206-209, 223.

Zuritz, C.A. and R.P. Singh, "Modeling Temperature Fluctuations in Stored Frozen Foods" *International Journal of Refrigeration,* 8 (1985): 289-293.

Zuritz, Carlos A. and Sudhir K. Sastry, "Effect of Packaging Materials on Temperature Fluctuations in Frozen Foods: Mathematical Model and Experimental Studies" *Journal of Food Science,* 51.4 (1986): 1050-1056.